Noname manuscript No.
(will be inserted by the editor)

Supplementary Online Material for Influence of Vessel Curvature and Plaque Composition on Drug Transport in the Arterial Wall following Drug-eluting Stent Implantation

Javier Escuer · Irene Aznar · Christopher McCormick · Estefanía Peña · Sean McGinty · Miguel A. Martínez

Received: date / Accepted: date

This document includes the following sections:

- S1. Supplemental equations
- S2. Supplemental figures
- S3. Supplemental tables

S1 Supplemental equations

S1.1 Kedem-Katchalsky equations for fluid flux

Endothelium (ET), internal and external elastic laminae (IEL and EEL, respectively) are treated as semipermeable membranes and the fluid flux across them, $J_{v,j}$, is described by the Kedem-Katchalsky equations [Kedem and Katchalsky, 1958]. Neglecting the osmotic contribution as an approximation [Formaggia et al., 2010; Bozsak et al., 2014; Escuer et al., 2020], the Kedem-Katchalsky equations for fluid flux can be simplified as:

$$J_{v,j} = L_{p,j} \Delta p_j, \tag{1}$$

where the subscript $j = \{et, etp, iel, ielp, eel\}$ denotes the semipermeable membranes considered: the lumen-SES interface (et), the lumen-plaque interface (etp), the SES-media interface (iel), the plaque-media interface (ielp) and the media-adventitia interface (eel), respectively; $L_{p,j}$ is the membrane hydraulic conductivity and; Δp_j the pressure drop across each semipermeable membrane. Therefore, the volume flux J_v for each membrane in case of healthy conditions (without plaque) in both inner and outer walls of the artery can be formulated as follows:

$$J_{v,et} = L_{p,et} \Delta p_{et} = L_{p,et}(p_l - p_{ses}), \tag{2}$$

$$J_{v,iel} = L_{p,iel} \Delta p_{iel} = L_{p,iel}(p_{ses} - p_m), \tag{3}$$

$$J_{v,eel} = L_{p,eel} \Delta p_{eel} = L_{p,eel}(p_m - p_a), \tag{4}$$

where l, ses, m and a denote the lumen, subendothelial space, media and adventitia, respectively. In the case of presence of plaque in the inner wall of the artery, the volume flux J_v in the boundaries corresponding to the plaque can be formulated as follows:

$$J_{v,etp} = L_{p,et} \Delta p_{etp} = L_{p,et}(p_l - p_{pfc}), \tag{5}$$

$$J_{v,ielp} = L_{p,iel} \Delta p_{iel} = L_{p,iel}(p_{pfc} - p_m), \tag{6}$$

where pfc denotes the plaque fibrous cap. In regions where the endothelium is considered denuded, the volume flux $J_{v,et}$ simplifies to continuity of pressure, i.e. $p_l = p_{ses}$ under healthy conditions or $p_l = p_{pfc}$ under unhealthy conditions.

J. Escuer
Aragón Institute for Engineering Research (I3A), University of Zaragoza, Spain.

I. Aznar
Aragón Institute for Engineering Research (I3A), University of Zaragoza, Spain.

C. McCormick
Department of Biomedical Engineering, University of Strathclyde, Glasgow, UK.

E. Peña
Aragón Institute for Engineering Research (I3A), University of Zaragoza, Spain.
Biomedical Research Networking Center in Bioengineering, Biomaterials and Nanomedicine (CIBER-BBN), Spain.

S. McGinty
Division of Biomedical Engineering, University of Glasgow, Glasgow, UK.

M. A. Martínez
Aragón Institute for Engineering Research (I3A), University of Zaragoza, Spain.
Biomedical Research Networking Center in Bioengineering, Biomaterials and Nanomedicine (CIBER-BBN), Spain.
María de Luna, 3. E-50018 Zaragoza (Spain).
E-mail: miguelam@unizar.es

S1.2 Kedem-Katchalsky equations for solute flux

Discontinuity of solute flux across the semipermeable membranes, $J_{s,j}$, is also governed by the Kedem-Katchalsky equations [Kedem and Katchalsky, 1958]:

$$J_{s,j} = P_j \Delta c_j + s_j \bar{c}_j J_{v,j}, \tag{7}$$

where P_j is the permeability of each semipermeable membrane; Δc_j is the solute concentration difference; s_j is the sieving coefficient and; $\bar{c}_j$ is the weighted average concentration on either side of the corresponding membrane computed as [Levitt, 1975; Bozsak et al., 2014; Escuer et al., 2020]:

$$\bar{c}_{et} = \frac{1}{2}(c_l + c_{ses}) + \frac{s_{et} J_{v,et}}{12 P_{et}}(c_l - c_{ses}), \tag{8}$$

$$\bar{c}_{etp} = \frac{1}{2}(c_l + c_{pfc}) + \frac{s_{et} J_{v,etp}}{12 P_{et}}(c_l - c_{pfc}), \tag{9}$$

$$\bar{c}_{iel} = \frac{1}{2}(c_{ses} + c_m) + \frac{s_{iel} J_{v,iel}}{12 P_{iel}}(c_{ses} - c_m), \tag{10}$$

$$\bar{c}_{ielp} = \frac{1}{2}(c_{pfc} + c_m) + \frac{s_{iel} J_{v,ielp}}{12 P_{iel}}(c_{pfc} - c_m), \tag{11}$$

$$\bar{c}_{eel} = \frac{1}{2}(c_m + c_{adv}) + \frac{s_{eel} J_{v,eel}}{12 P_{eel}}(c_m - c_{adv}). \tag{12}$$

Therefore, the solute flux J_s for each membrane in case of healthy conditions (without plaque) in both inner and outer walls of the artery can be formulated as follows:

$$J_{s,et} = P_{et}(c_l - c_{ses}) + s_{et} \bar{c}_{et} J_{v,et}, \tag{13}$$

$$J_{s,iel} = P_{iel}(c_{ses} - c_m) + s_{iel} \bar{c}_{iel} J_{v,iel}, \tag{14}$$

$$J_{s,eel} = P_{eel}(c_m - c_a) + s_{eel} \bar{c}_{eel} J_{v,eel}. \tag{15}$$

In the case of presence of plaque in the inner wall of the artery, the volume flux J_v in the boundaries corresponding to the plaque can be formulated as follows:

$$J_{s,etp} = P_{et}(c_l - c_{pfc}) + s_{et} \bar{c}_{etp} J_{v,etp}, \tag{16}$$

$$J_{s,ielp} = P_{iel}(c_{pfc} - c_m) + s_{iel} \bar{c}_{ielp} J_{v,ielp}. \tag{17}$$

S2 Suplemental figures

In Fig. S1 we present the temporal variation of NMC of sirolimus within each layer of the arterial wall obtained for the simulations corresponding to the straight artery ($\kappa = 0$) and five different degrees of curvature ($\kappa = 0.025 - 0.4$) under healthy conditions (without plaque) considering a timescale of 30 days. Since binding is only considered in the media, in Fig. S2 we separate-out free NMC from bound NMC (both specific and non-specific) in this layer.

[Fig. 1 about here.]

[Fig. 2 about here.]

The corresponding spatially varying profiles of free, specific (S) bound and non-specific (NS) bound normalised local concentration (NLC) of sirolimus, calculated as c_i/C_0, b_i^s/C_0 and b_i^{ns}/C_0, respectively, at four different time points (10 minutes, 1 hour, 4 hour and 1 day) after stent implantation are shown in this section (Figs. S3 - S5). Six cases of arterial curvature are compared under healthy arterial wall conditions. The results are shown in a radial section between the middle struts. These figures complement the results presented in Figs. 7 and 8 in the *Results* section of the main document, which are related with the study of the effect of vessel curvature on spatial drug distribution in the tissue.

[Fig. 3 about here.]

[Fig. 4 about here.]

[Fig. 5 about here.]

In Figs. S6 - S7 we display spatial profiles of target receptor (specific) and ECM (non-specific) binding site saturation levels.

[Fig. 6 about here.]

[Fig. 7 about here.]

To study the local concentrations throughout the different regions of the arterial wall, not only in representative sections such as a radial section between the middle stent struts, our model also enables us to generate useful 2D plots of the spatial distribution of drug for the first 7 days after DES implantation. In Fig. S8 we compare the spatial distribution of the drug for two curvature ratios ($\kappa = 0.1$ and $\kappa = 0.4$) in the outer wall of the artery. This figure complement the results presented in Fig. 8 of the main document where we plot the spatial variation of total NLC across the inner wall tissue domain showing clear differences in drug deposition, with the higher curvature leading to higher NLC of drug, with the effect most prominent at early times.

[Fig. 8 about here.]

In Figs. S9 - S13 the spatial distributions of total NLC of sirolimus at five different time points for each curvature ratio (from $\kappa = 0.025$ to $\kappa = 0.4$) in the inner and the outer wall are shown.

[Fig. 9 about here.]

[Fig. 10 about here.]

[Fig. 11 about here.]

[Fig. 12 about here.]

[Fig. 13 about here.]

Regarding the analysis of the influence of plaque composition on drug transport within the arterial wall, the temporal distribution of the free and bound NMC of drug in different regions of the inner wall of the artery are shown in Figs. S14 and S15, respectively. Three different plaque core compositions are compared: fibrotic, lipid and calcified. In Fig. S16, we also show the results corresponding to the percentage of binding sites that are saturated as a function of time.

[Fig. 14 about here.]

[Fig. 15 about here.]

[Fig. 16 about here.]

We also represent the spatially-varying profiles of free and bound NLC of sirolimus and the binding site % saturation in the inner wall of the artery at four different time points (Figs. S17 - S21). The results are shown for three different plaque core compositions: fibrotic, lipid and calcified for a curvature ratio of $\kappa = 0.1$ (average curvature ratio). Moreover, the results for the straight model ($\kappa = 0$) and for a curvature ratio of $\kappa = 0.1$, both under healthy conditions (i.e. healthy vessel without plaque) are shown.

[Fig. 17 about here.]

[Fig. 18 about here.]

[Fig. 19 about here.]

[Fig. 20 about here.]

[Fig. 21 about here.]

We show a 2D plot with the spatial distribution of the NLC of sirolimus in the inner wall of the artery under unhealthy conditions (in presence of plaque) at five time points for a curvature ratio of $\kappa = 0.1$. (Fig. S22). Figs. S14 - S22 complement the results presented in Figs. 9 and 10 which can be found in the *Results* section of the main document.

[Fig. 22 about here.]

Although the results presented in this work are focussed on the drug distribution in the arterial wall, we also show a 2D plot with the spatial distribution of the NLC of sirolimus in the lumen for two different curvature ratios ($\kappa = 0.1$ and $\kappa = 0.4$). We can observe that the drug concentration in the blood is about 3-4 orders of magnitude lower than in the tissue.

[Fig. 23 about here.]

Finally, we calculated the following non-dimensional parameters: the Dean number ($De_l = Re_l\sqrt{\kappa}$) for the flow in the curved vessel and the radial Peclet number ($Pe_{r,i1} = u_{r,i1}\delta_{i1}/D_{r,i1}$) for transport in the wall. It can be noted a nonlinear increase in Dean number with curvature (Fig. S24) and consequent asymmetry in the fluid flow pattern in the lumen (Fig. S25). In Fig. S26 we plot the magnitude of the radial component of the plasma filtration velocity and the radial Peclet number across the inner and outer walls of the artery, respectively, for the different cases of curvature considered under healthy conditions.

[Fig. 24 about here.]

[Fig. 25 about here.]

[Fig. 26 about here.]

S3 Suplemental tables

The maximum values of normalised local concentrations (NLC) in each region of the tissue at six different time points for the different cases simulated are shown in Tables S1 and S2.

[Table 1 about here.]

[Table 2 about here.]

Acknowledgements This work was funded by the Spanish Ministry of Economy, Industry and Competitiveness through research project number DPI2016-76630-C2-1-R and grant number BES-2014-069737; the Department of Industry and Innovation (Government of Aragon) through research group grant number T24-17R (Fondo Social Europeo) and research project number LMP121-18 and; the Carlos III Health Institute (ISCIII) through the CIBER initiative. Dr. McGinty acknowledges funding provided by EPSRC (Grant number EP/S030875/1).

Conflict of interest The authors declare that they have no conflict of interest.

References

Bozsak F, Chomaz JM, Barakat AI (2014) Modeling the transport of drugs eluted from stents: physical phenomena driving drug distribution in the arterial wall. Biomechanics and Modeling in Mechanobiology 13(2):327–347

Escuer J, Cebollero M, Peña E, McGinty S, Martínez MA (2020) How does stent expansion alter drug transport properties of the arterial wall? Journal of the Mechanical Behavior of Biomedical Materials p 103610

Formaggia L, Quarteroni A, Veneziani A (2010) Cardiovascular Mathematics: Modeling and simulation of the circulatory system, vol 1. Springer Science & Business Media

Kedem O, Katchalsky A (1958) Thermodynamic analysis of the permeability of biological membranes to non-electrolytes. Biochimica et Biophysica Acta 27:229–246

Levitt DG (1975) General continuum analysis of transport through pores. i. proof of onsager's reciprocity postulate for uniform pore. Biophysical Journal 15(6):533–551

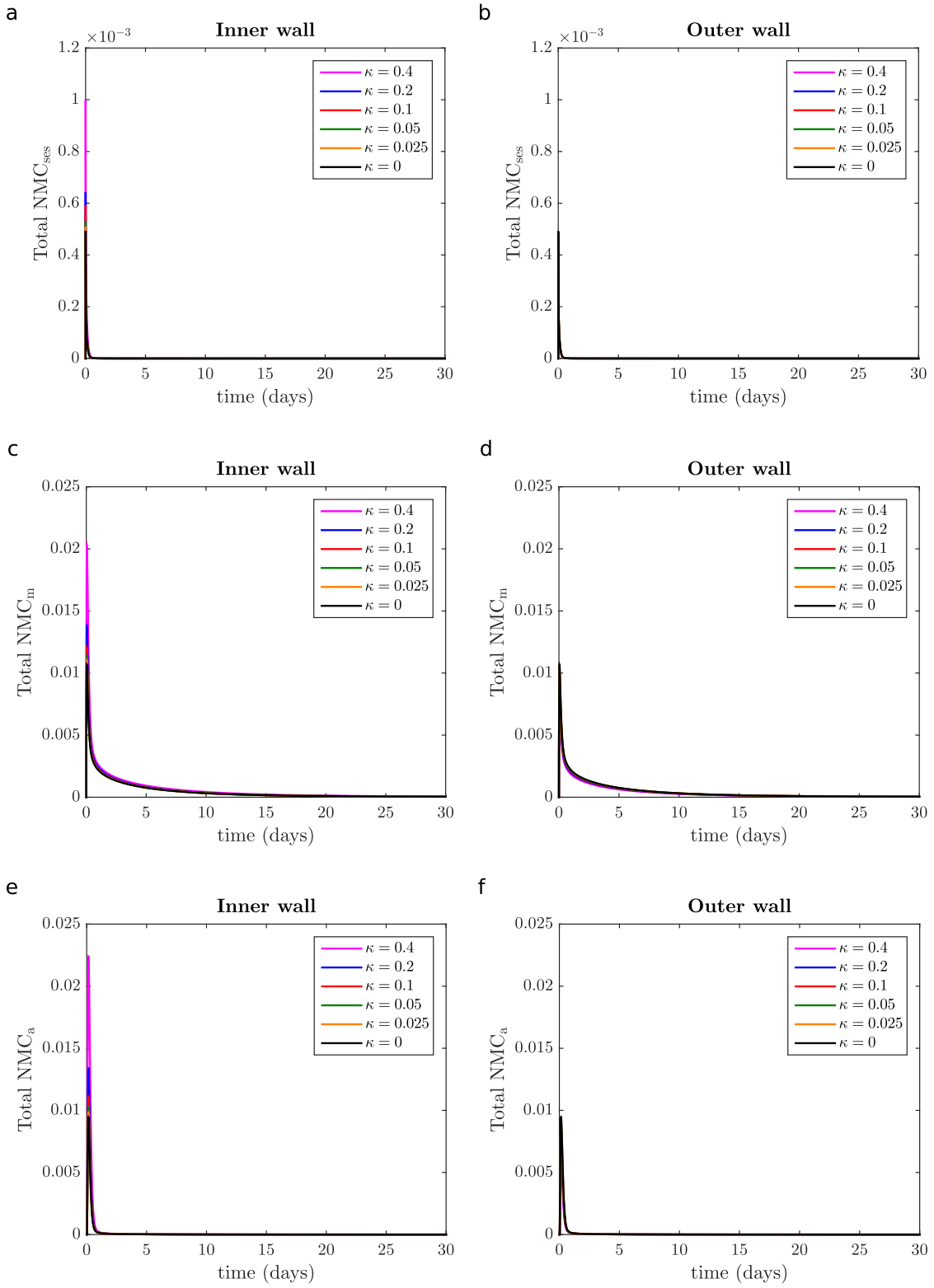

Fig. S1 Time-varying profiles of total normalised mean concentration (NMC) of sirolimus in each layer of the inner and outer wall of the artery: SES (a, b); media (c, d) and adventitia (e, f). The results are shown for the straight model ($\kappa = 0$) and for five different degrees of arterial curvature ($\kappa = 0.025 - 0.4$). The timescale of all the plots is 30 days. These figures complement the results presented in Figs. 4 and 5 in the *Results* section of the main document.

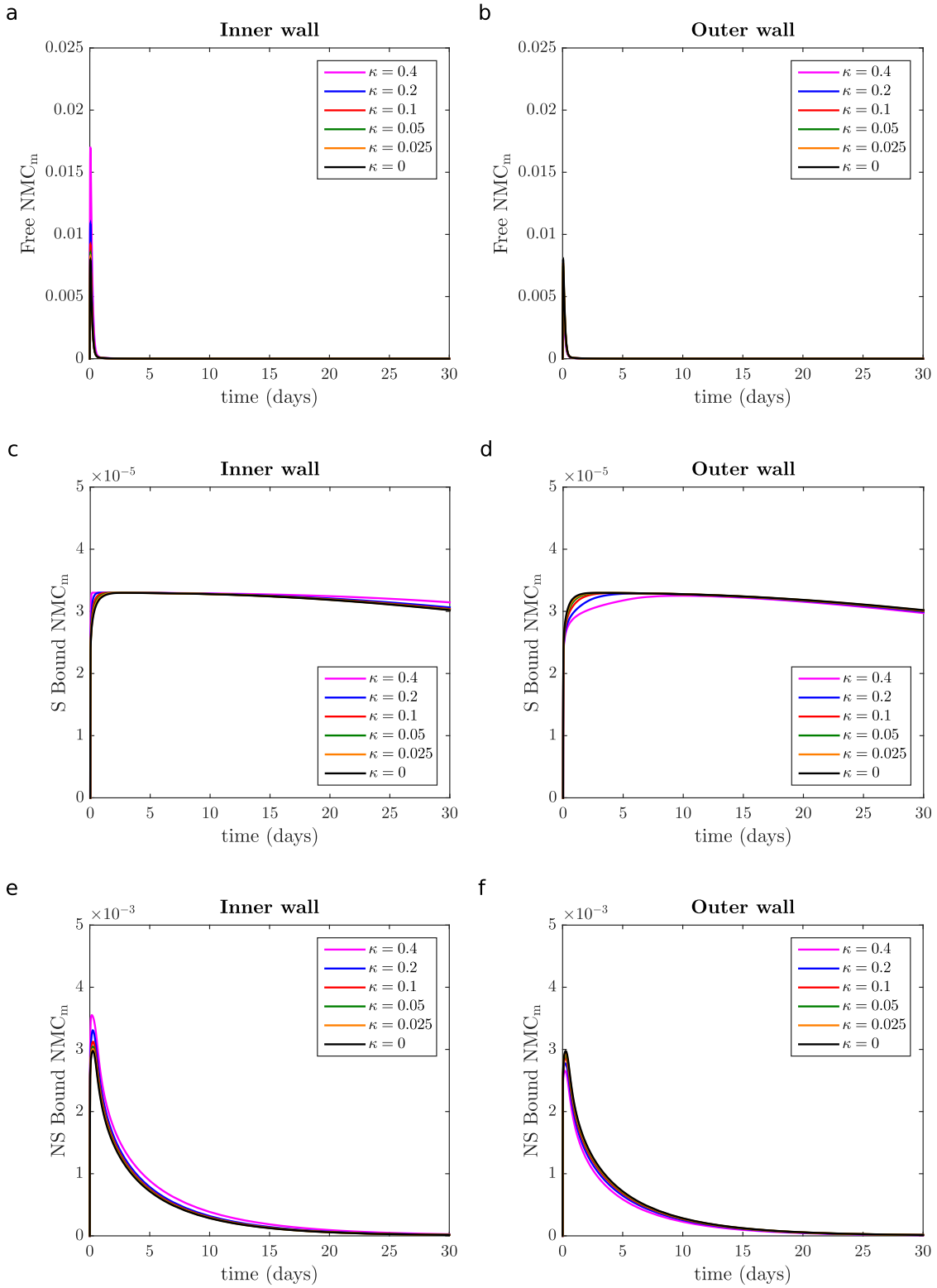

Fig. S2 Time-varying profiles of free and bound (specific and non-specific) normalised mean concentration (NMC) of sirolimus in the media layer of the inner and outer wall of the artery: free NMC (a, b); specific bound NMC (c, d) and non-specific bound (e, f). The results are shown for the straight model ($\kappa = 0$) and for five different degrees of arterial curvature ($\kappa = 0.025 - 0.4$). Note the different scales on the y-axes in subfigures c, d, e and f compared with subfigures a and b and the previous figure (Fig. S1). The timescale of all the plots is 30 days. These figures complement the results presented in Figs. 4 and 5 in the *Results* section of the main document.

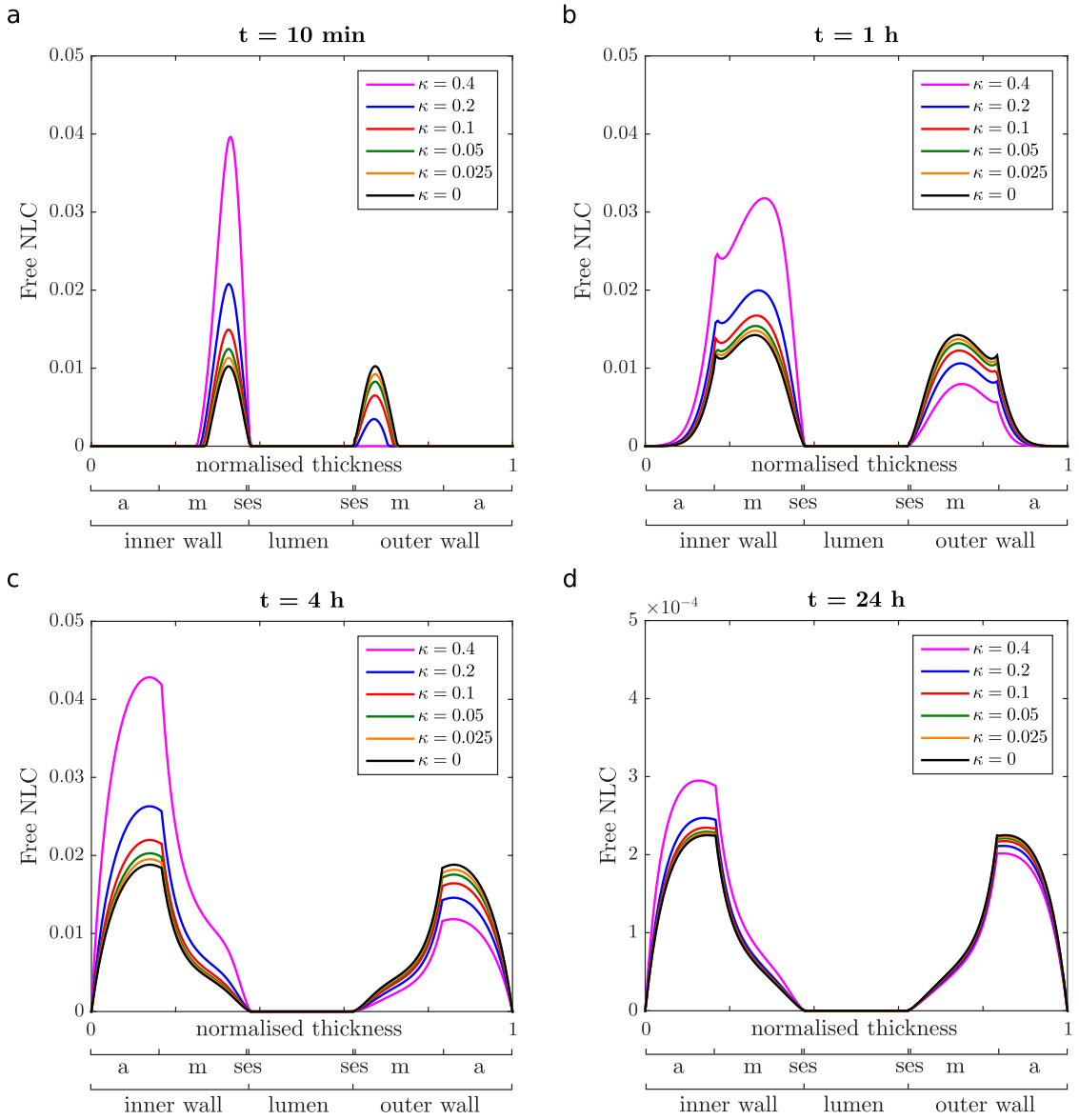

Fig. S3 Spatially varying profiles of free normalised local concentration (NLC) of sirolimus in the tissue, calculated as c_i/C_0, at 10 min (a), 1 hour (b), 4 hours (c) and 1 day (d) after stent implantation. The results are shown for the straight model ($\kappa = 0$) and for five different degrees of arterial curvature ($\kappa = 0.025 - 0.4$) in a radial section between the middle stent struts. Note the different scale on the y-axis in subfigure d. Note also that lumen diameter is not drawn to scale.

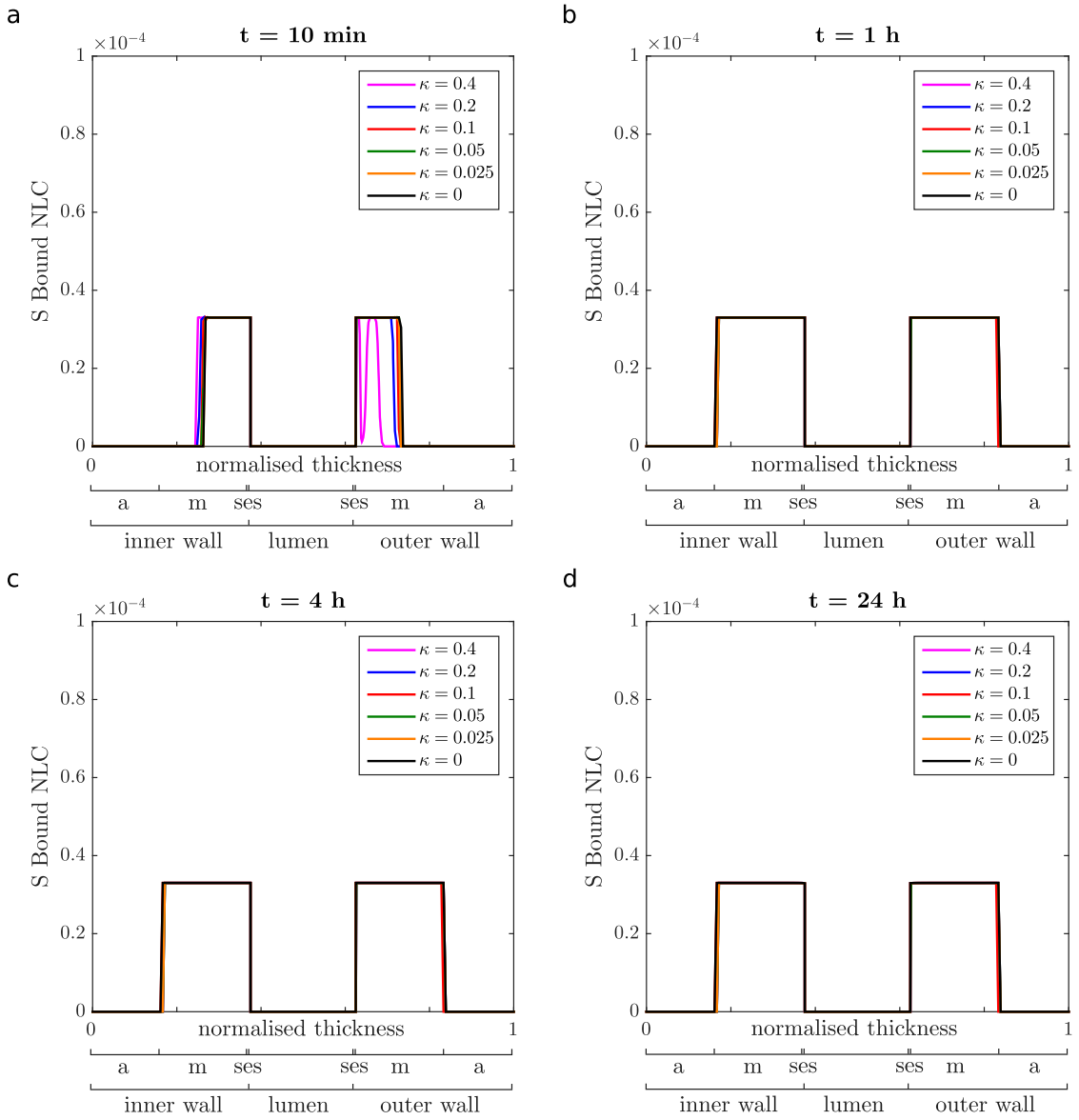

Fig. S4 Spatially varying profiles of specific bound normalised local concentration (NLC) of sirolimus in the tissue, calculated as b_i^s/C_0, at 10 min (a), 1 hour (b), 4 hours (c) and 1 day (d) after stent implantation. The results are shown for the straight model ($\kappa = 0$) and for five different degrees of arterial curvature ($\kappa = 0.025 - 0.4$) in a radial section between the middle stent struts. Note that there is different scale on the y-axes compared with Fig. 7 of the main document. Note also that lumen diameter is not drawn to scale.

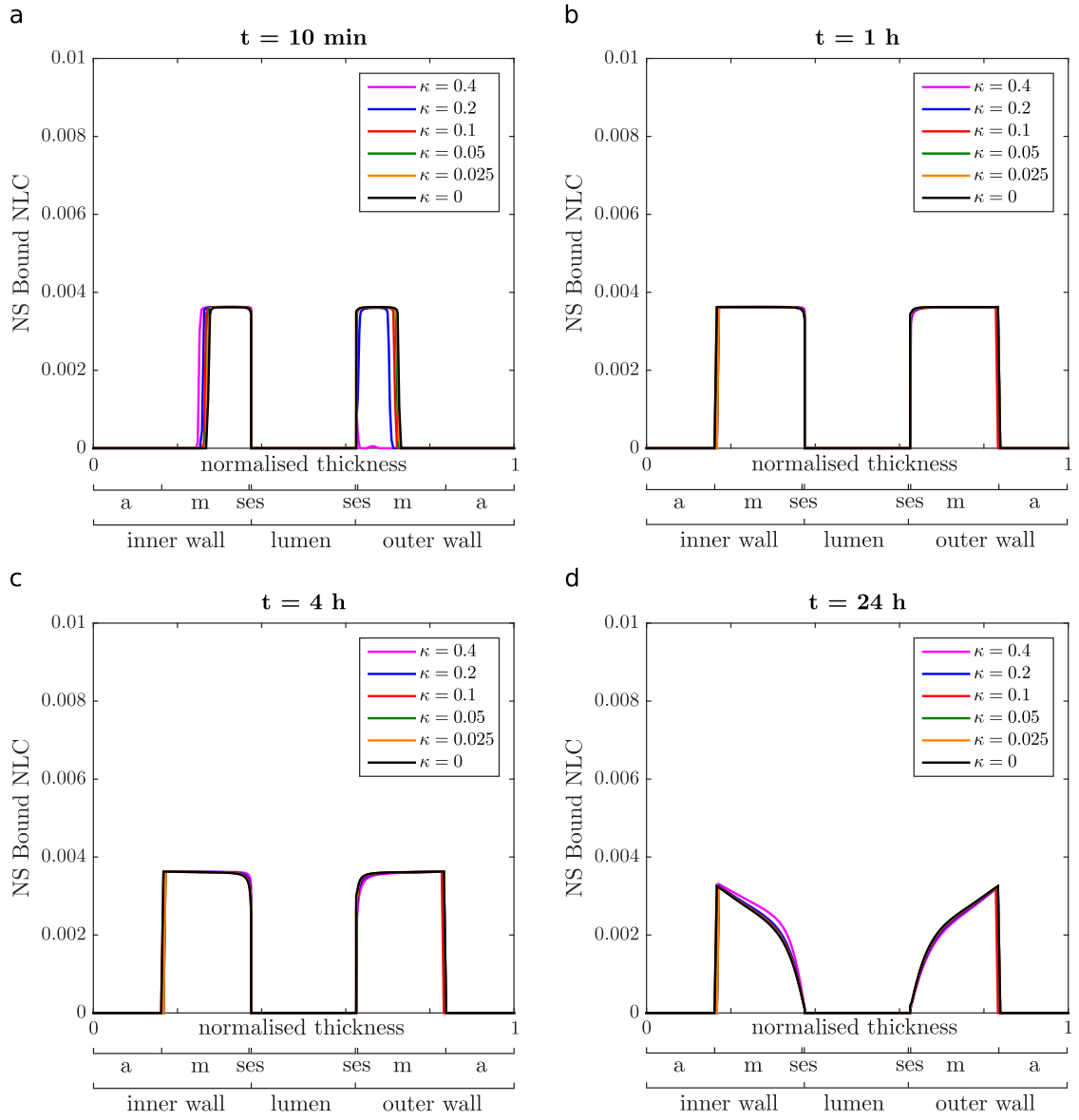

Fig. S5 Spatially varying profiles of non-specific bound normalised local concentration (NLC) of sirolimus in the tissue, calculated as b_i^{ns}/C_0, at 10 min (a), 1 hour (b), 4 hours (c) and 1 day (d) after stent implantation. The results are shown for the straight model ($\kappa = 0$) and for five different degrees of arterial curvature ($\kappa = 0.025 - 0.4$) in a radial section between the middle stent struts. Note that there is different scale on the y-axes compared with Fig. 7 of the main document. Note also that lumen diameter is not drawn to scale.

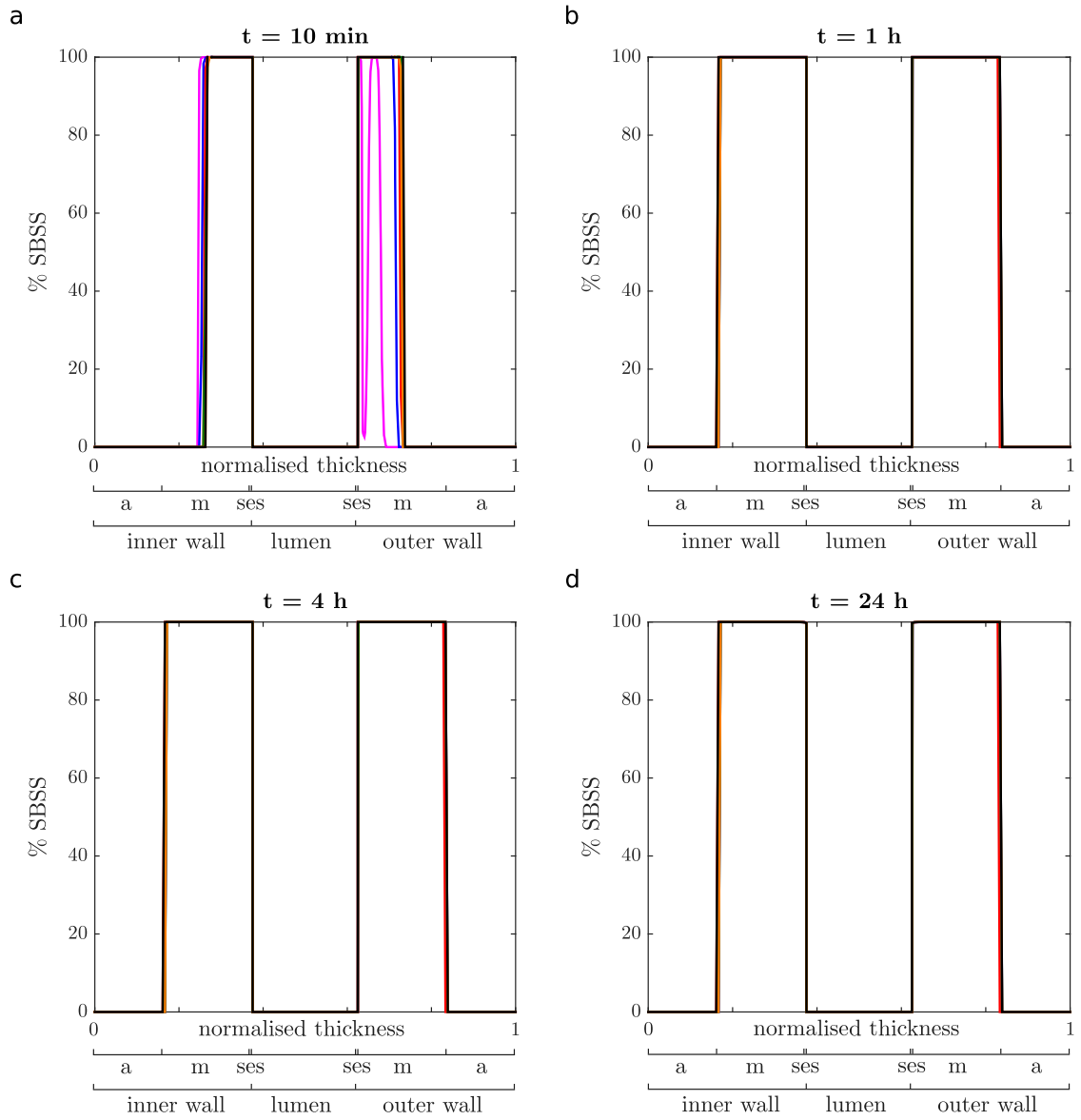

Fig. S6 Spatially varying profiles of target receptor binding site % saturation of sirolimus in the tissue, calculated as $b_i^s/C_0 \cdot 100$, at 10 min (a), 1 hour (b), 4 hours (c) and 1 day (d) after stent implantation. The results are shown for the straight model ($\kappa = 0$) and for five different degrees of arterial curvature ($\kappa = 0.025 - 0.4$) in a radial section between the middle stent struts. Note that lumen diameter is not drawn to scale.

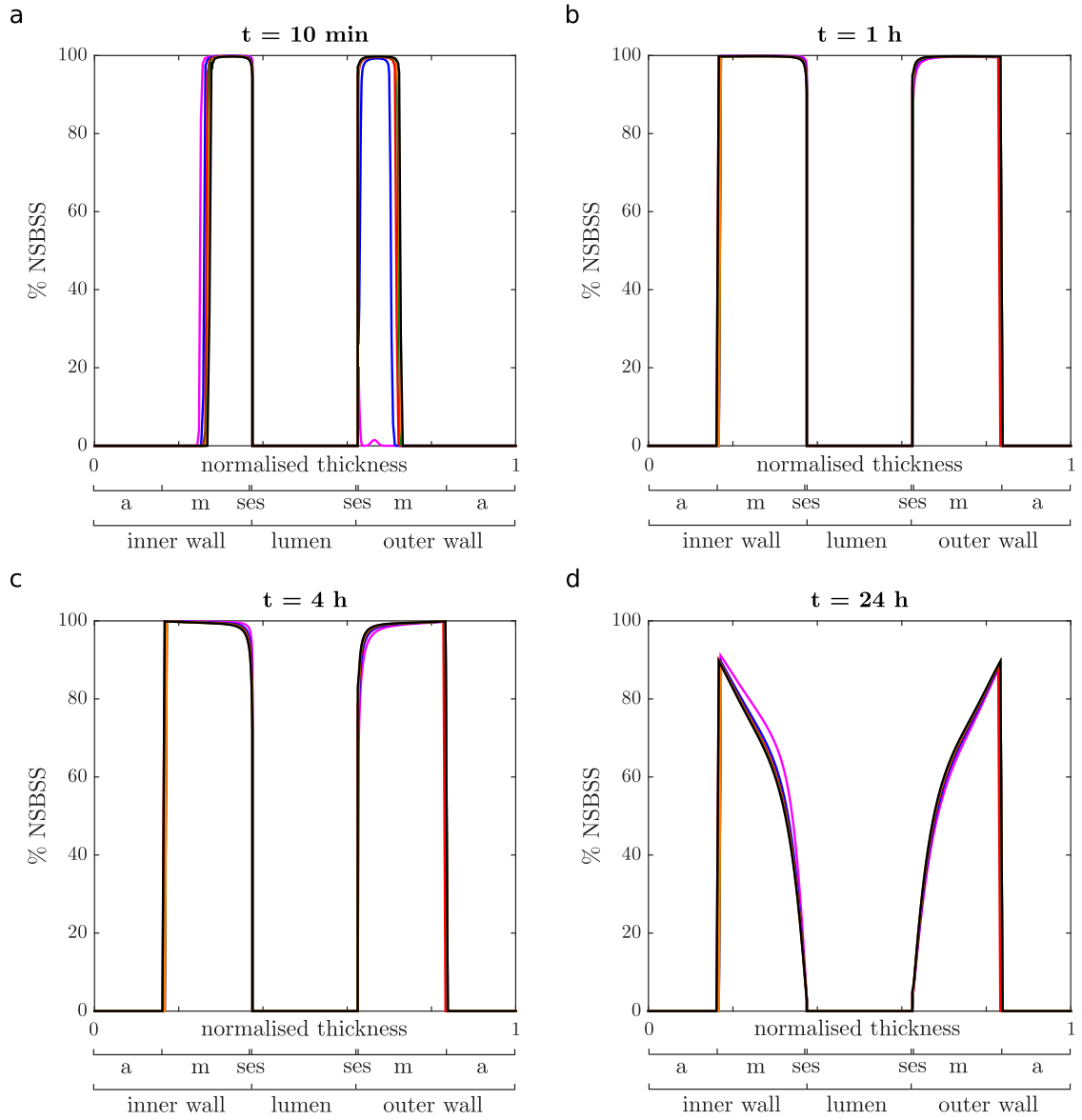

Fig. S7 Spatially varying profiles of ECM binding site % saturation of sirolimus in the tissue, calculated as $b_i^{ns}/C_0 \cdot 100$, at 10 min (a), 1 hour (b), 4 hours (c) and 1 day (d) after stent implantation. The results are shown for the straight model ($\kappa = 0$) and for five different degrees of arterial curvature ($\kappa = 0.025 - 0.4$) in a radial section between the middle stent struts. Note that lumen diameter is not drawn to scale.

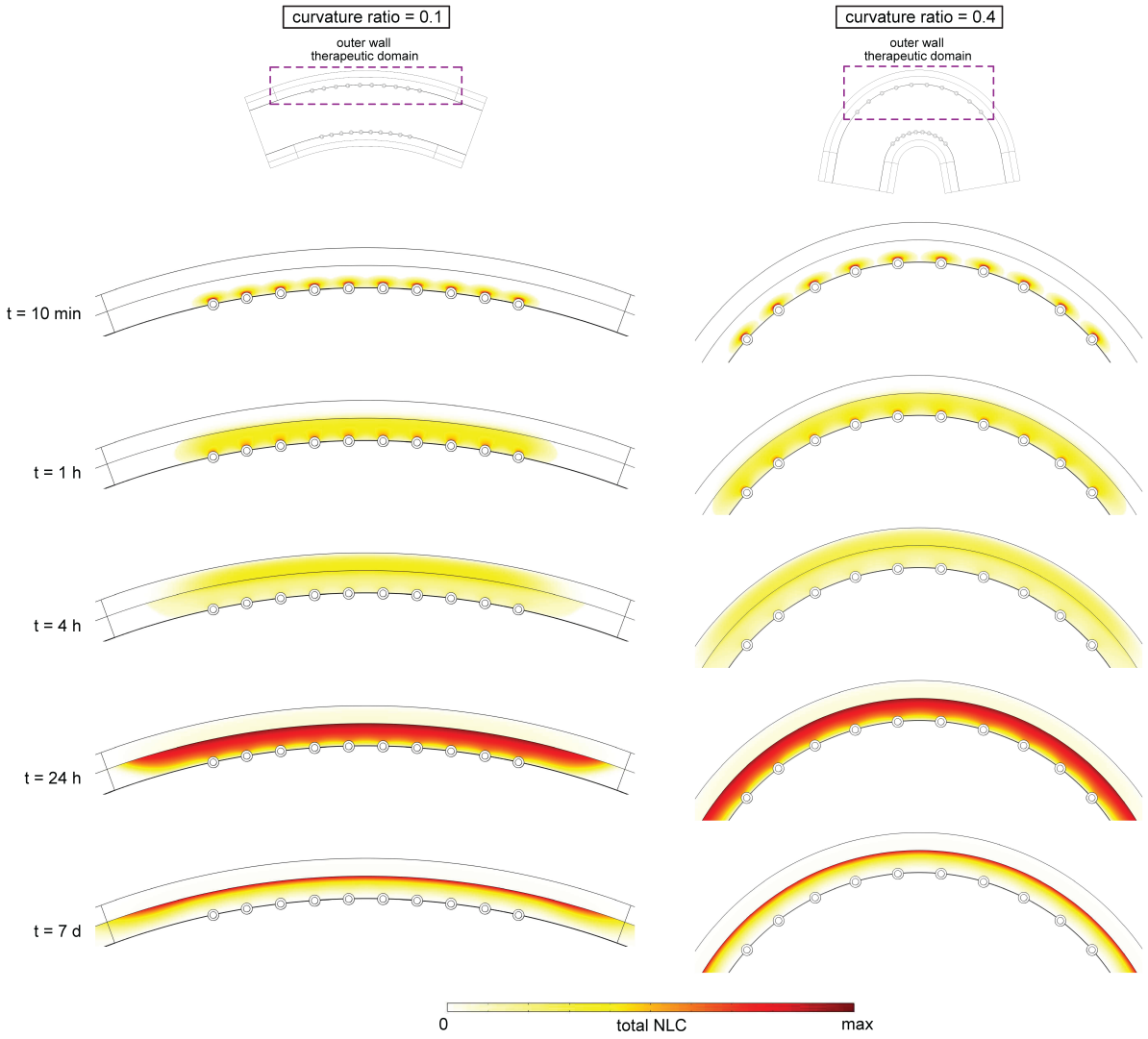

Fig. S8 Spatial variation of total NLC of sirolimus, calculated as $(c_i + b_i^s + b_i^{ns})/C_0$, within the outer wall of the artery at five different time points (t = 10 min, t = 1 hour, t = 4 hours, t = 24 hours and t = 7 days) for curvature ratios of $\kappa = 0.1$ (average curvature ratio) and $\kappa = 0.4$, respectively. For each time point the same colour scale is used for both cases. The maximum values of total NLC of drug chosen for each time point are the following: max $= 6.23 \cdot 10^{-2}$ at t = 10 min; max $= 4.16 \cdot 10^{-2}$ at t = 1 h; max $= 4.56 \cdot 10^{-2}$ at t = 4 h; max $= 3.65 \cdot 10^{-3}$ at t = 24 h and; max $= 1.74 \cdot 10^{-3}$ at t = 7 d. Tables with the maximum values at each time point for all cases considered may be found in Section S3 (Table S1) of this Supplementary Material.

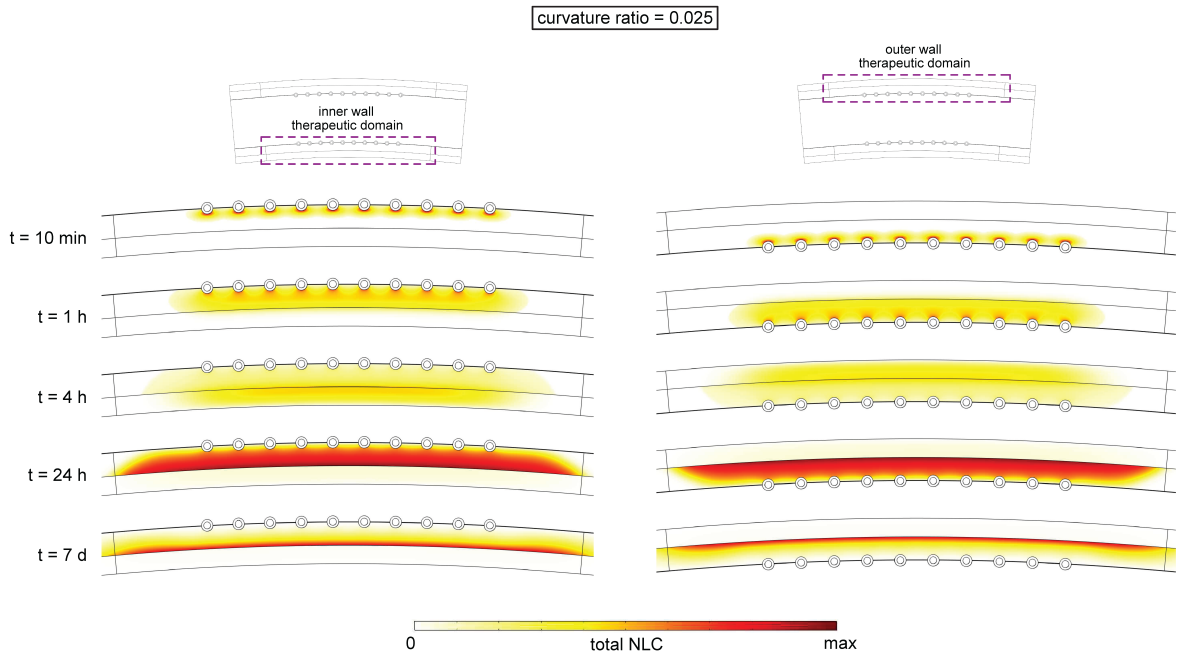

Fig. S9 Spatial variation of total NLC of sirolimus, calculated as $(c_i + b_i^s + b_i^{ns})/C_0$, at five different time points (t = 10 min, t = 1 hour, t = 4 hours, t = 24 hours and t = 7 days) for a curvature ratio of $\kappa = 0.025$ in the inner and the outer wall, respectively. For each time point the same colour scale is used for both cases. The maximum values of total NLC of drug chosen for each time point are the following: max = $6.23 \cdot 10^{-2}$ at t = 10 min; max = $4.16 \cdot 10^{-2}$ at t = 1 h; max = $4.56 \cdot 10^{-2}$ at t = 4 h; max = $3.65 \cdot 10^{-3}$ at t = 24 h and; max = $1.74 \cdot 10^{-3}$ at t = 7 d. Tables with the maximum values at each time point for all cases considered may be found in Section S3 (Table S1) of this Supplementary Material.

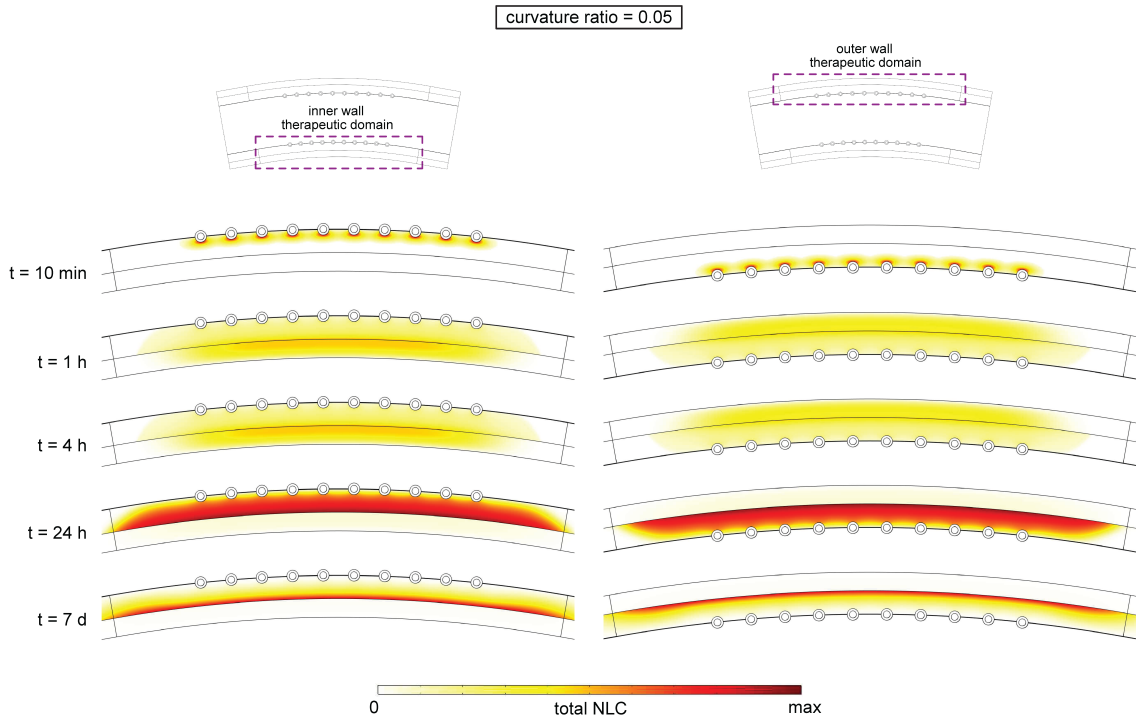

Fig. S10 Spatial variation of total NLC of sirolimus, calculated as $(c_i + b_i^s + b_i^{ns})/C_0$, at five different time points (t = 10 min, t = 1 hour, t = 4 hours, t = 24 hours and t = 7 days) for a curvature ratio of $\kappa = 0.05$ in the inner and the outer wall, respectively. For each time point the same colour scale is used for both cases. The maximum values of total NLC of drug chosen for each time point are the following: max $= 6.23 \cdot 10^{-2}$ at t = 10 min; max $= 4.16 \cdot 10^{-2}$ at t = 1 h; max $= 4.56 \cdot 10^{-2}$ at t = 4 h; max $= 3.65 \cdot 10^{-3}$ at t = 24 h and; max $= 1.74 \cdot 10^{-3}$ at t = 7 d. Tables with the maximum values at each time point for all cases considered may be found in Section S3 (Table S1) of this Supplementary Material.

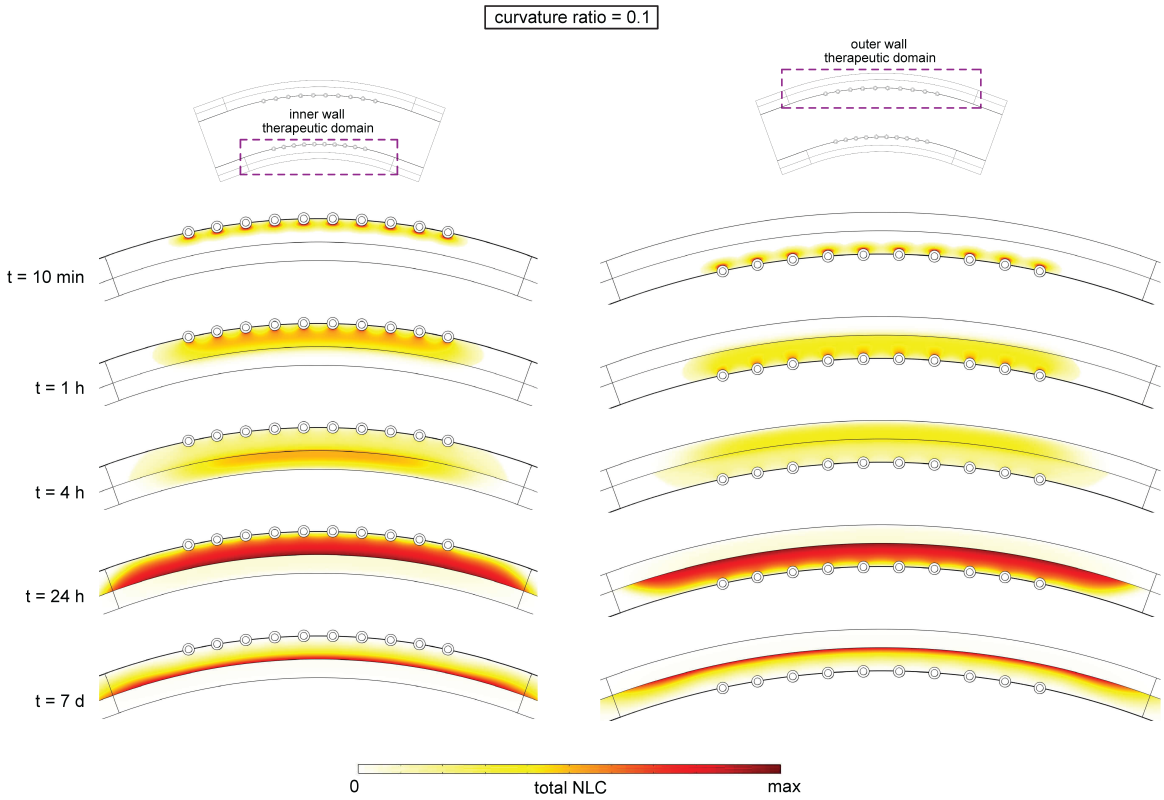

Fig. S11 Spatial variation of total NLC of sirolimus, calculated as $(c_i + b_i^s + b_i^{ns})/C_0$, at five different time points (t = 10 min, t = 1 hour, t = 4 hours, t = 24 hours and t = 7 days) for a curvature ratio of $\kappa = 0.1$ (average curvature ratio) in the inner and the outer wall, respectively. For each time point the same colour scale is used for both cases. The maximum values of total NLC of drug chosen for each time point are the following: max = $6.23 \cdot 10^{-2}$ at t = 10 min; max = $4.16 \cdot 10^{-2}$ at t = 1 h; max = $4.56 \cdot 10^{-2}$ at t = 4 h; max = $3.65 \cdot 10^{-3}$ at t = 24 h and; max = $1.74 \cdot 10^{-3}$ at t = 7 d. Tables with the maximum values at each time point for all cases considered may be found in Section S3 (Table S1) of this Supplementary Material.

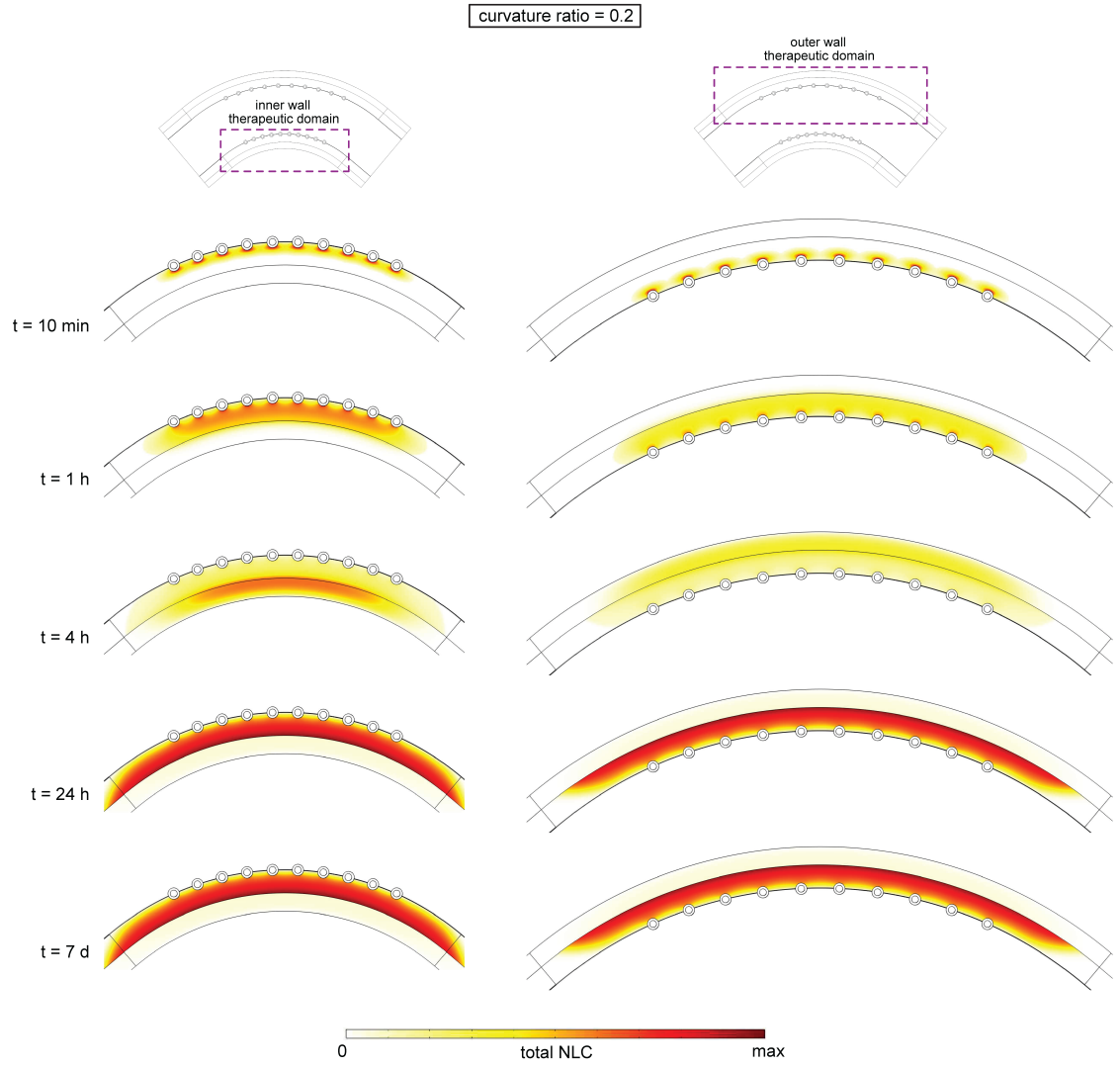

Fig. S12 Spatial variation of total NLC of sirolimus, calculated as $(c_i + b_i^s + b_i^{ns})/C_0$, at five different time points (t = 10 min, t = 1 hour, t = 4 hours, t = 24 hours and t = 7 days) for a curvature ratio of $\kappa = 0.2$ in the inner and the outer wall, respectively. For each time point the same colour scale is used for both cases. The maximum values of total NLC of drug chosen for each time point are the following: max = $6.23 \cdot 10^{-2}$ at t = 10 min; max = $4.16 \cdot 10^{-2}$ at t = 1 h; max = $4.56 \cdot 10^{-2}$ at t = 4 h; max = $3.65 \cdot 10^{-3}$ at t = 24 h and; max = $1.74 \cdot 10^{-3}$ at t = 7 d. Tables with the maximum values at each time point for all cases considered may be found in Section S3 (Table S1) of this supplementary material.

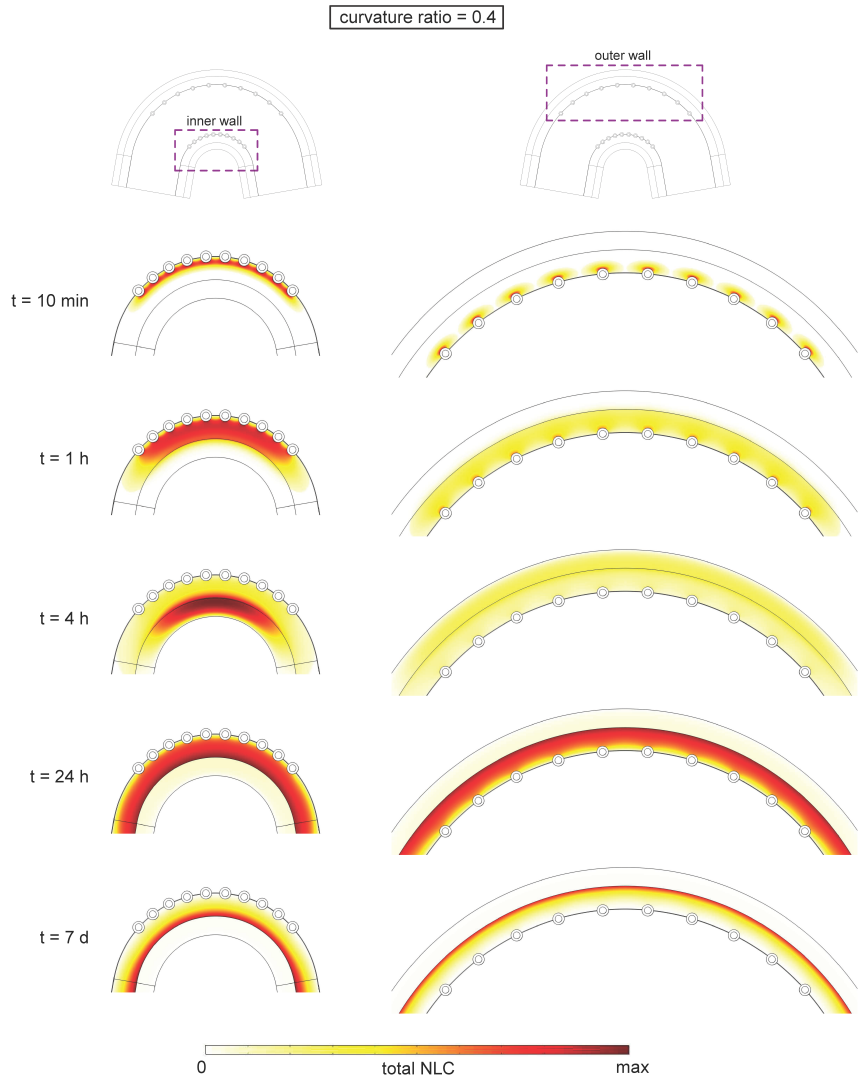

Fig. S13 Spatial variation of total NLC of sirolimus, calculated as $(c_i + b_i^s + b_i^{ns})/C_0$, at five different time points (t = 10 min, t = 1 hour, t = 4 hours, t = 24 hours and t = 7 days) for a curvature ratio of $\kappa = 0.4$ in the inner and the outer wall, respectively. For each time point the same colour scale is used for both cases. The maximum values of total NLC of drug chosen for each time point are the following: max = $6.23 \cdot 10^{-2}$ at t = 10 min; max = $4.16 \cdot 10^{-2}$ at t = 1 h; max = $4.56 \cdot 10^{-2}$ at t = 4 h; max = $3.65 \cdot 10^{-3}$ at t = 24 h and; max = $1.74 \cdot 10^{-3}$ at t = 7 d. Tables with the maximum values at each time point for all cases considered may be found in Section S3 (Table S1) of this Supplementary Material.

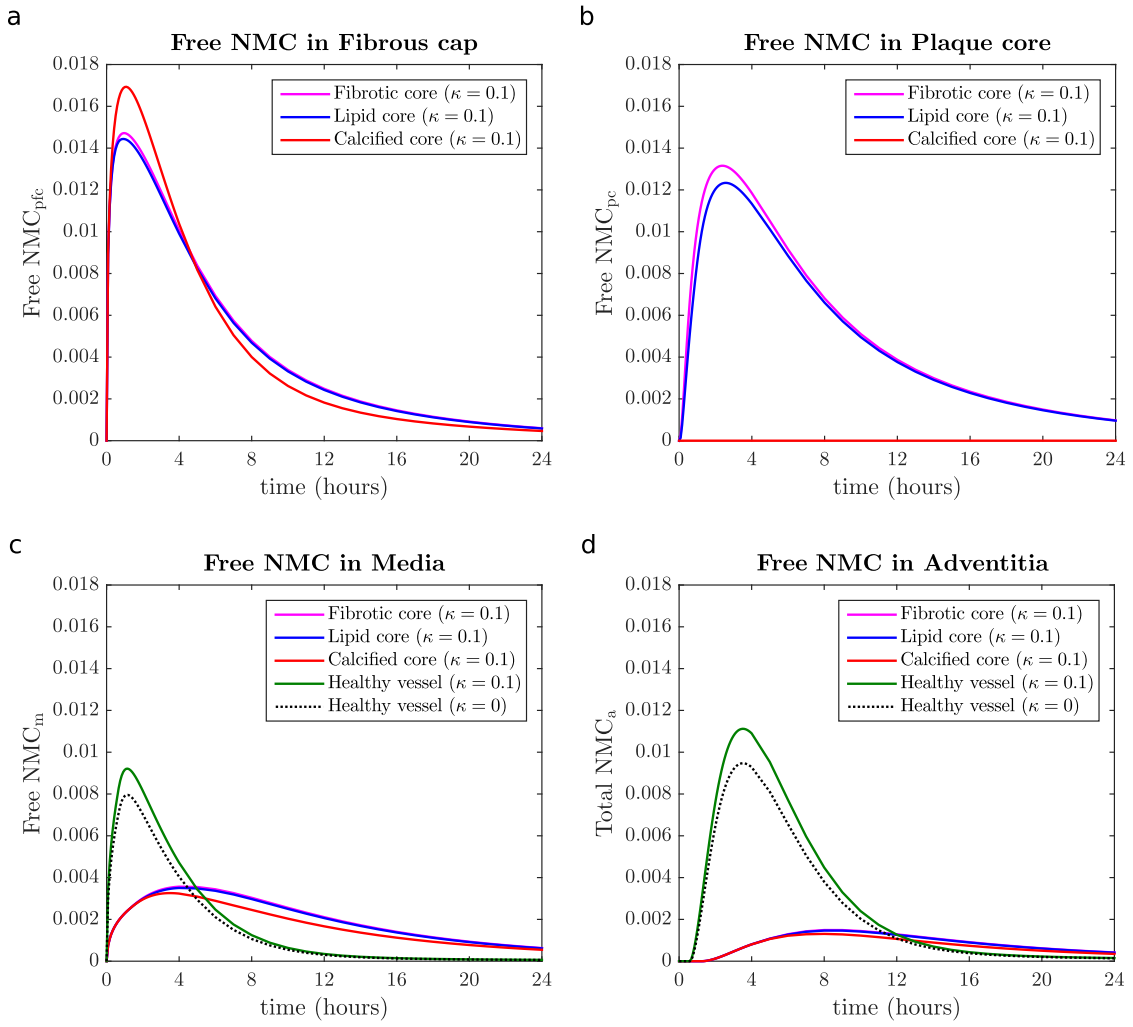

Fig. S14 Time-varying profiles of free NMC of sirolimus in the fibrous cap (a), plaque core (b), media (c) and adventitia (d) within the inner wall of the artery for a curvature ratio of $\kappa = 0.1$ (average curvature ratio). The results are shown for three different plaque core compositions: fibrotic, lipid and calcified. In case of the media and adventitia, the results are also shown for the straight model ($\kappa = 0$) and for a curvature ratio of $\kappa = 0.1$, both under healthy conditions (i.e. healthy vessel without plaque).

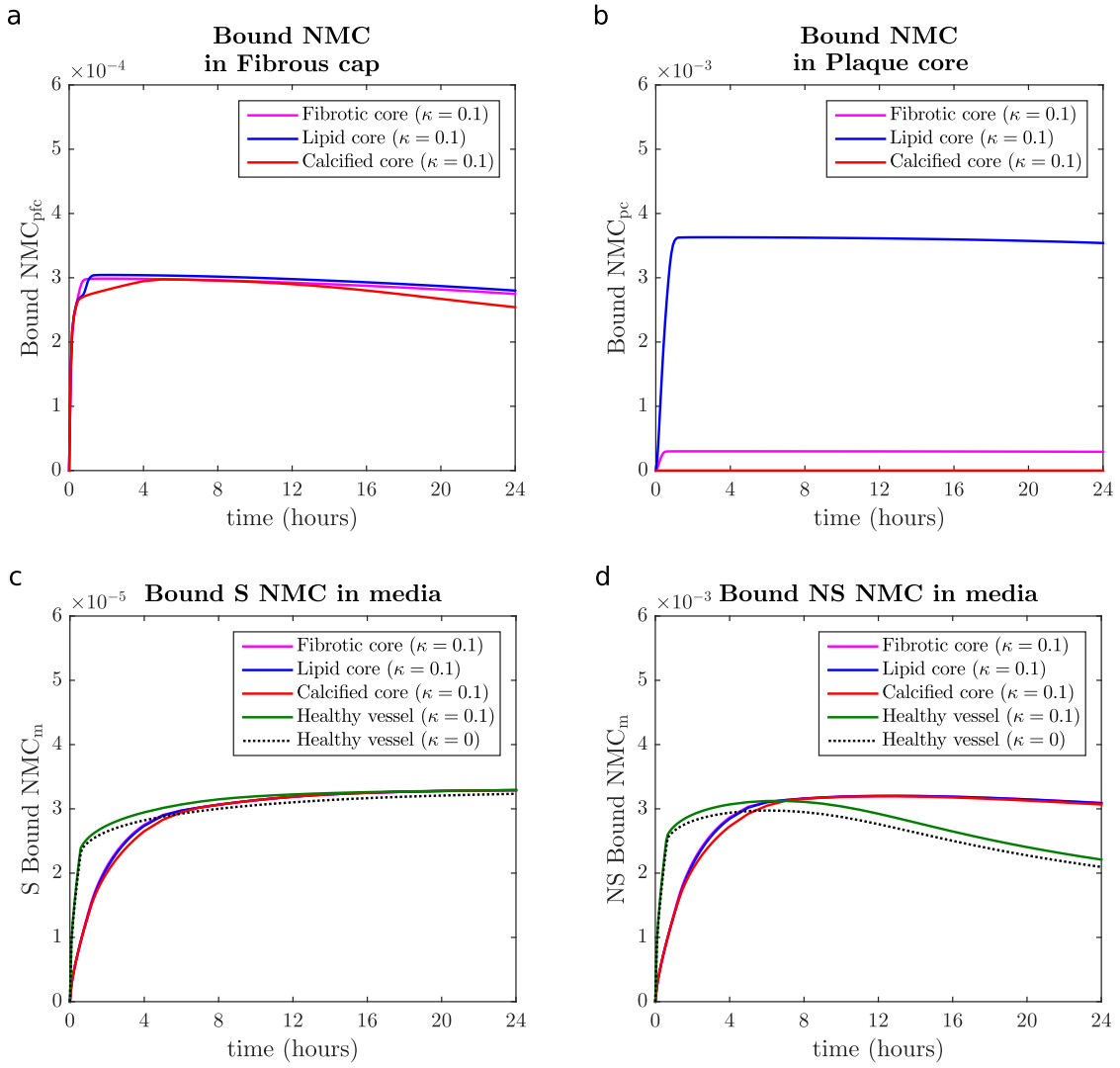

Fig. S15 Time-varying profiles of bound NMC of sirolimus in the plaque regions: fibrous cap (a) and core (b), and specific and non-specific bound NMC in the media (c, d) within the inner wall of the artery for a curvature ratio of $\kappa = 0.1$ (average curvature ratio). The results are shown for three different plaque core compositions: fibrotic, lipid and calcified. In case of the media, the results are also shown for the straight model ($\kappa = 0$) and for a curvature ratio of $\kappa = 0.1$, both under healthy conditions (i.e. healthy vessel without plaque). Note that there are different scales on the y-axes on all plots compared with the previous figure (Fig. S14) and Fig. 9 of the main document.

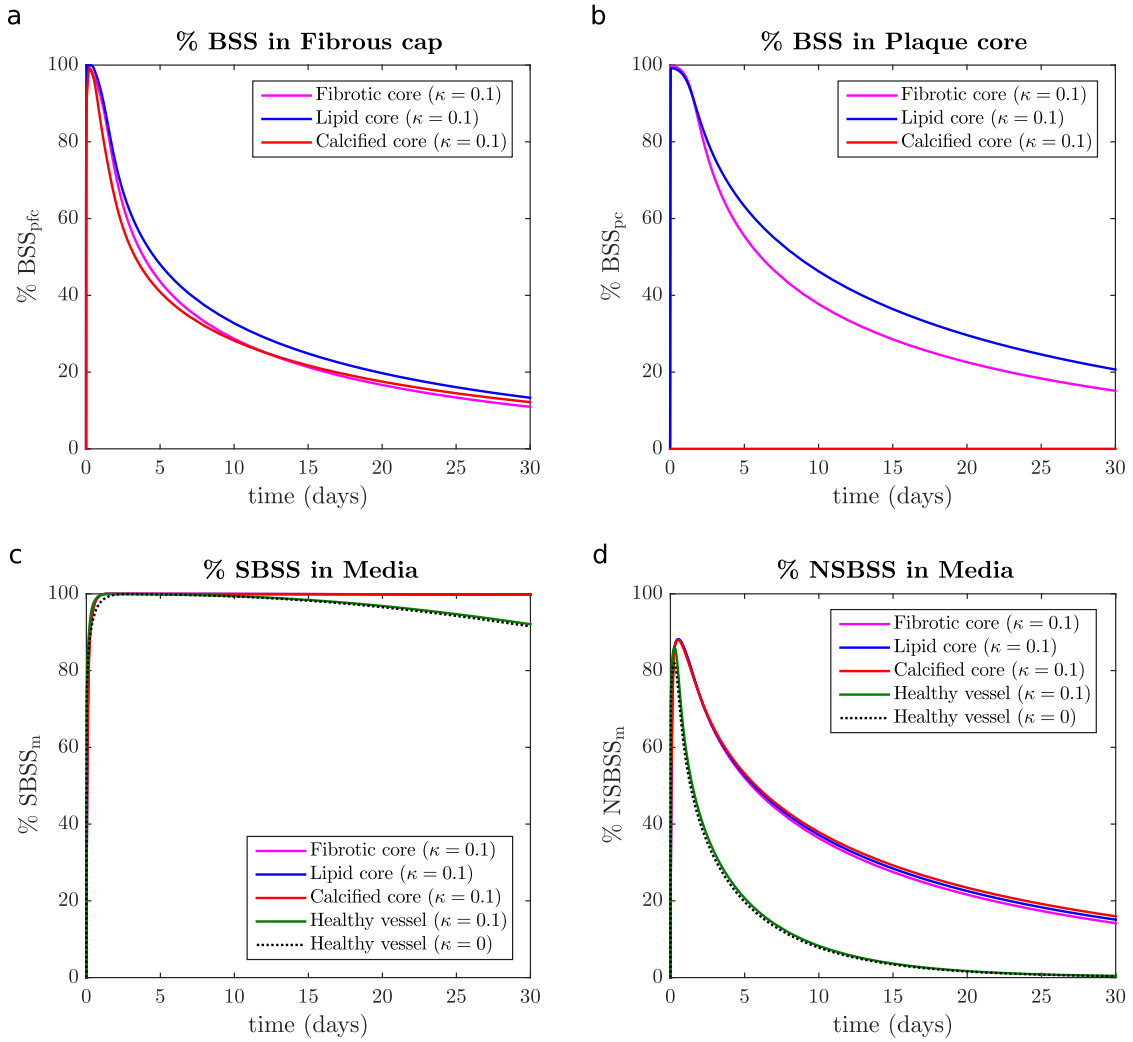

Fig. S16 Time-varying profiles of the binding site % saturation in the plaque regions: fibrous cap (a) and core (b), and specific and non-specific binding site % saturation in the media (c, d) within the inner wall of the artery for a curvature ratio of $\kappa = 0.1$ (average curvature ratio). The results are shown for three different plaque core compositions: fibrotic, lipid and calcified. In case of the media, the results are also shown for the straight model ($\kappa = 0$) and for a curvature ratio of $\kappa = 0.1$, both under healthy conditions (i.e. healthy vessel without plaque).

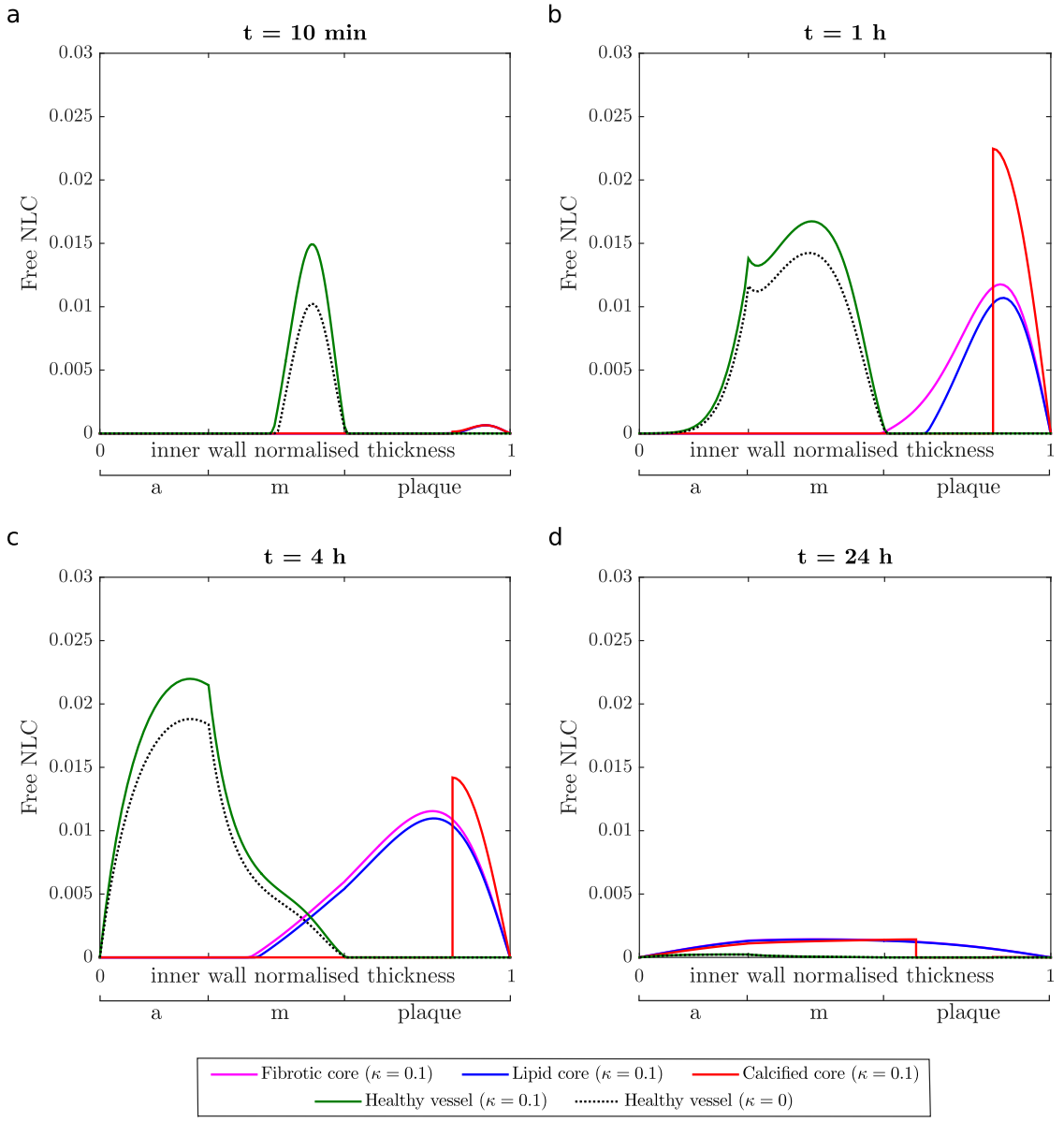

Fig. S17 Spatially varying profiles of free NLC of sirolimus, calculated as c_i/C_0, in the inner wall of the artery at 10 min (a), 1 hour (b), 4 hours (c) and 1 day (d) after stent implantation in a radial section between the middle stent struts. The results are shown for three different plaque core compositions: fibrotic, lipid and calcified for a curvature ratio of $\kappa = 0.1$ (average curvature ratio). Moreover, the results for the straight model ($\kappa = 0$) and for a curvature ratio of $\kappa = 0.1$, both under healthy conditions (i.e. healthy vessel without plaque) are shown.

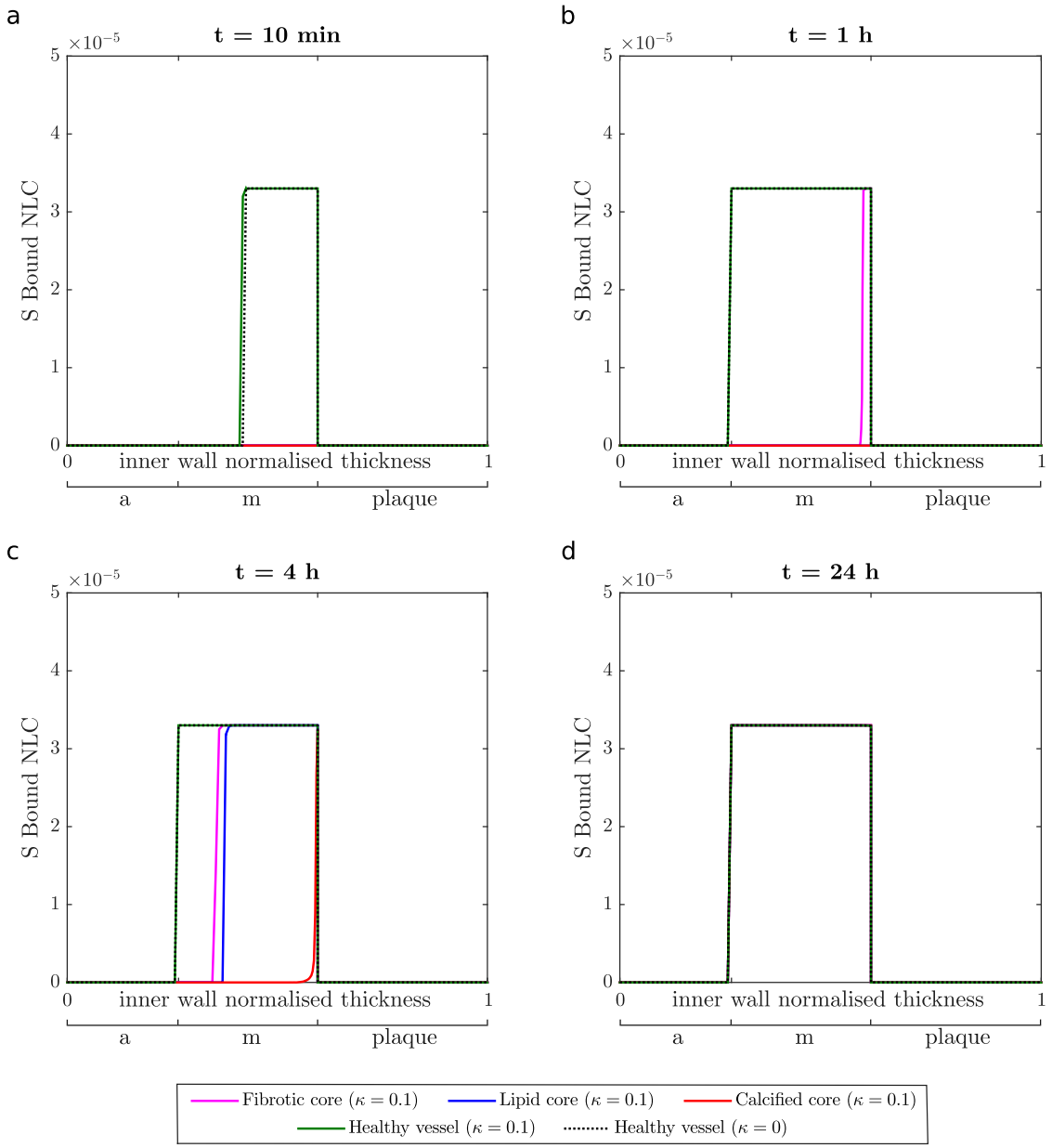

Fig. S18 Spatially varying profiles of specific (S) bound NLC of sirolimus, calculated as b_i^s/C_0, in the inner wall of the artery at 10 min (a), 1 hour (b), 4 hours (c) and 1 day (d) after stent implantation in a radial section between the middle stent struts. The results are shown for three different plaque core compositions: fibrotic, lipid and calcified for a curvature ratio of $\kappa = 0.1$ (average curvature ratio). Moreover, the results for the straight model ($\kappa = 0$) and for a curvature ratio of $\kappa = 0.1$, both under healthy conditions (i.e. healthy vessel without plaque) are shown. Note that there is different scale on the y-axes compared with the previous figure (Fig. S17) and Fig. 10 of the main document.

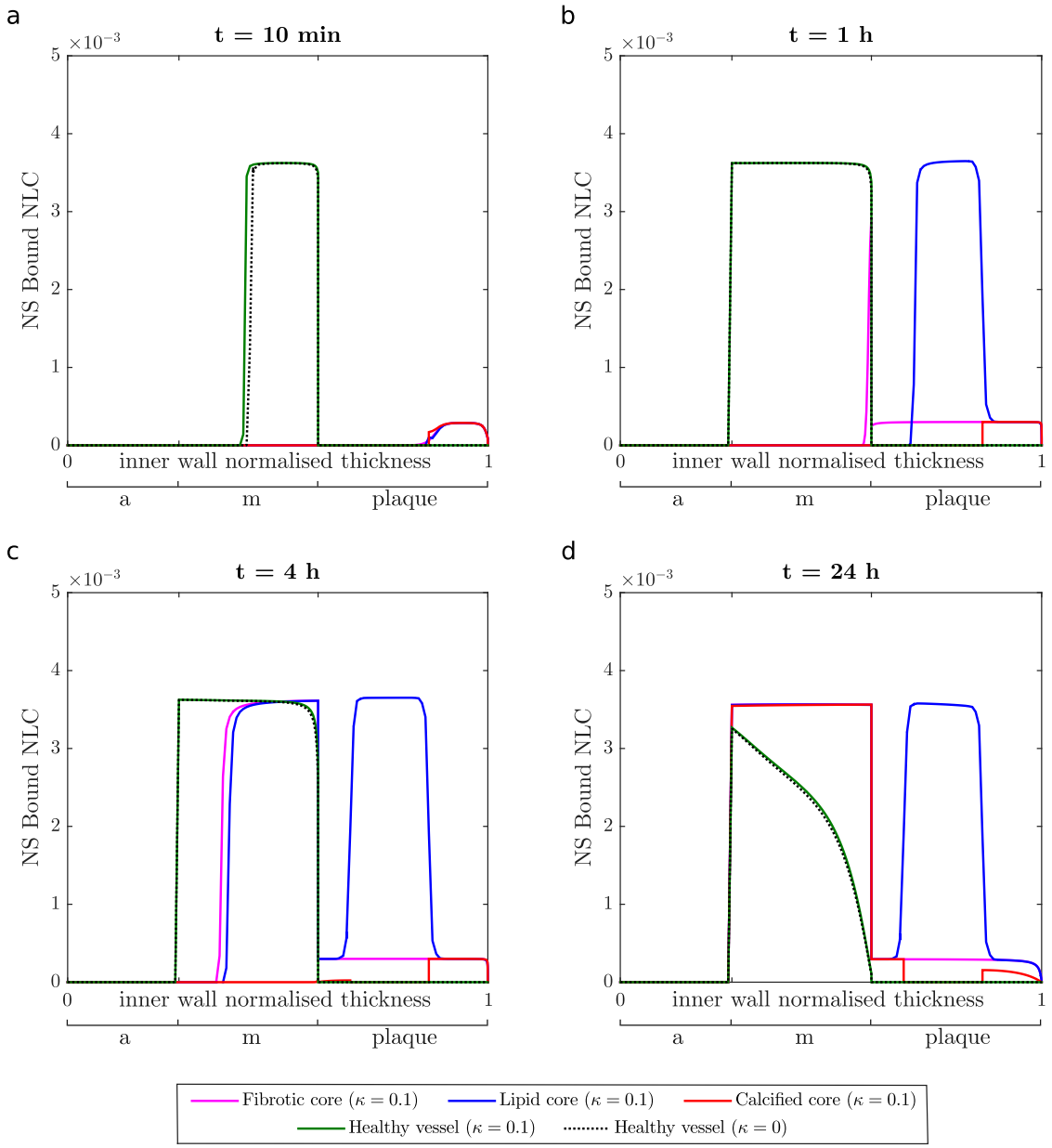

Fig. S19 Spatially varying profiles of non-specific (NS) bound NLC of sirolimus, calculated as b_i^{ns}/C_0, in the inner wall of the artery at 10 min (a), 1 hour (b), 4 hours (c) and 1 day (d) after stent implantation in a radial section between the middle stent struts. The results are shown for three different plaque core compositions: fibrotic, lipid and calcified for a curvature ratio of $\kappa = 0.1$ (average curvature ratio). Moreover, the results for the straight model ($\kappa = 0$) and for a curvature ratio of $\kappa = 0.1$, both under healthy conditions (i.e. healthy vessel without plaque) are shown. Note that there is different scale on the y-axes compared with the two previous figures (Figs. S17 and S18) and Fig. 10 of the main document.

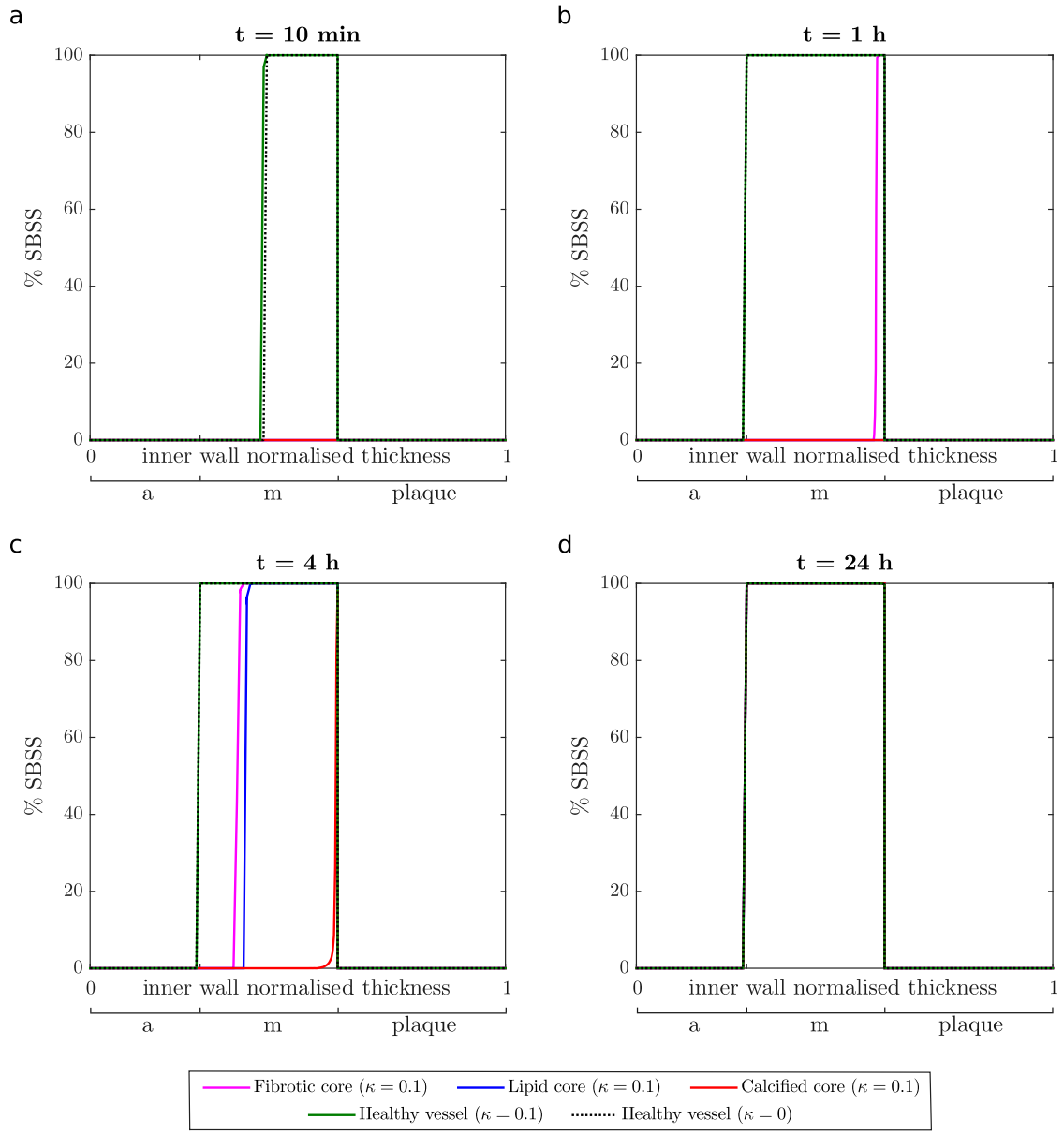

Fig. S20 Spatially varying profiles of specific (S) binding site % saturation in the inner wall of the artery, calculated as $(b_i^s/b_{max,i}^s)\cdot 100$, at 10 min (a), 1 hour (b), 4 hours (c) and 1 day (d) after stent implantation in a radial section between the middle stent struts. The results are shown for three different plaque core compositions: fibrotic, lipid and calcified for a curvature ratio of $\kappa = 0.1$ (average curvature ratio). Moreover, the results for the straight model ($\kappa = 0$) and for a curvature ratio of $\kappa = 0.1$, both under healthy conditions (i.e. healthy vessel without plaque) are shown.

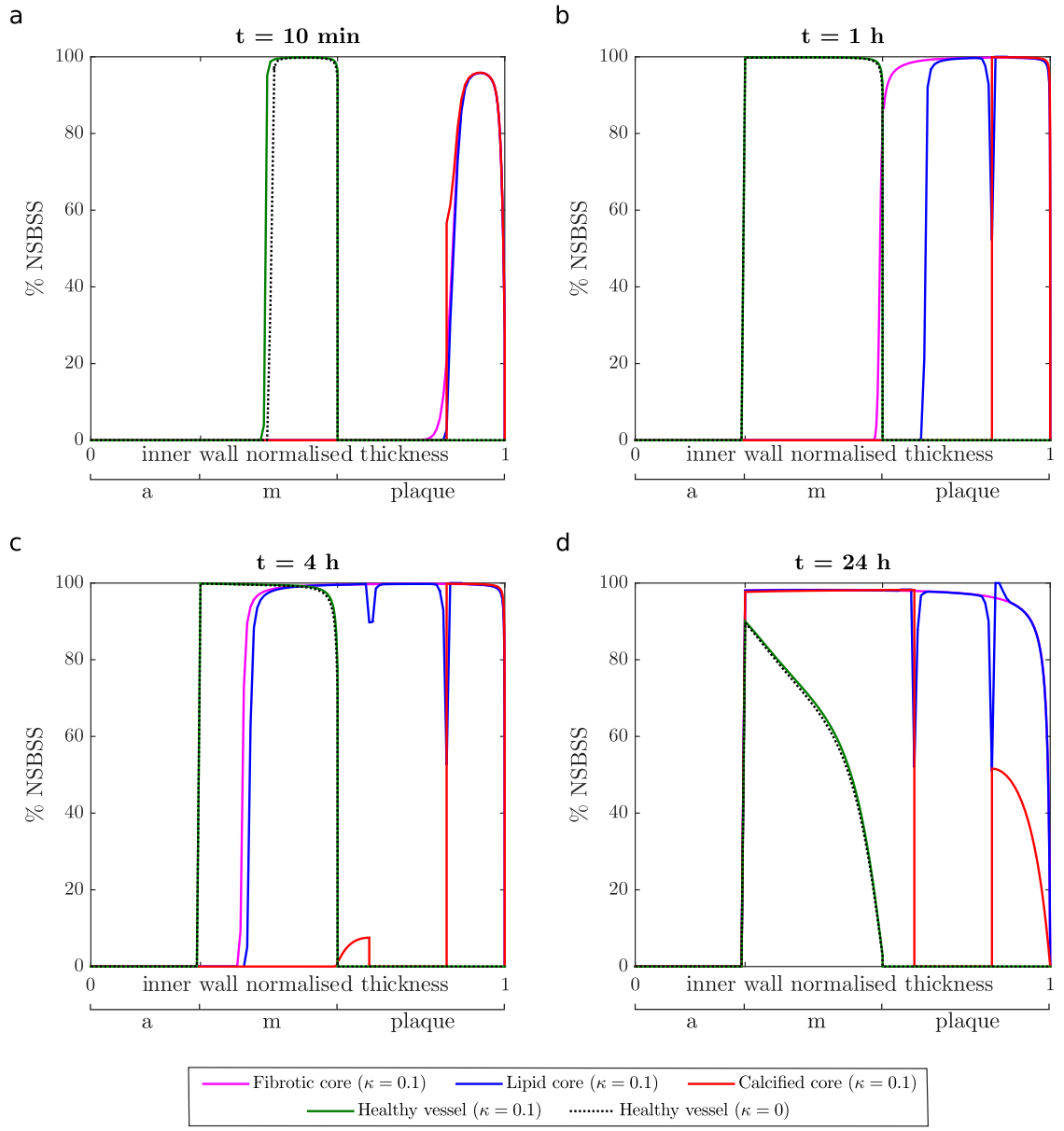

Fig. S21 Spatially varying profiles of specific (NS) binding site % saturation in the inner wall of the artery, calculated as $(b_i^{ns}/b_{max,i}^{ns}) \cdot 100$, at 10 min (a), 1 hour (b), 4 hours (c) and 1 day (d) after stent implantation in a radial section between the middle stent struts. The results are shown for three different plaque core compositions: fibrotic, lipid and calcified for a curvature ratio of $\kappa = 0.1$ (average curvature ratio). Moreover, the results for the straight model ($\kappa = 0$) and for a curvature ratio of $\kappa = 0.1$, both under healthy conditions (i.e. healthy vessel without plaque) are shown.

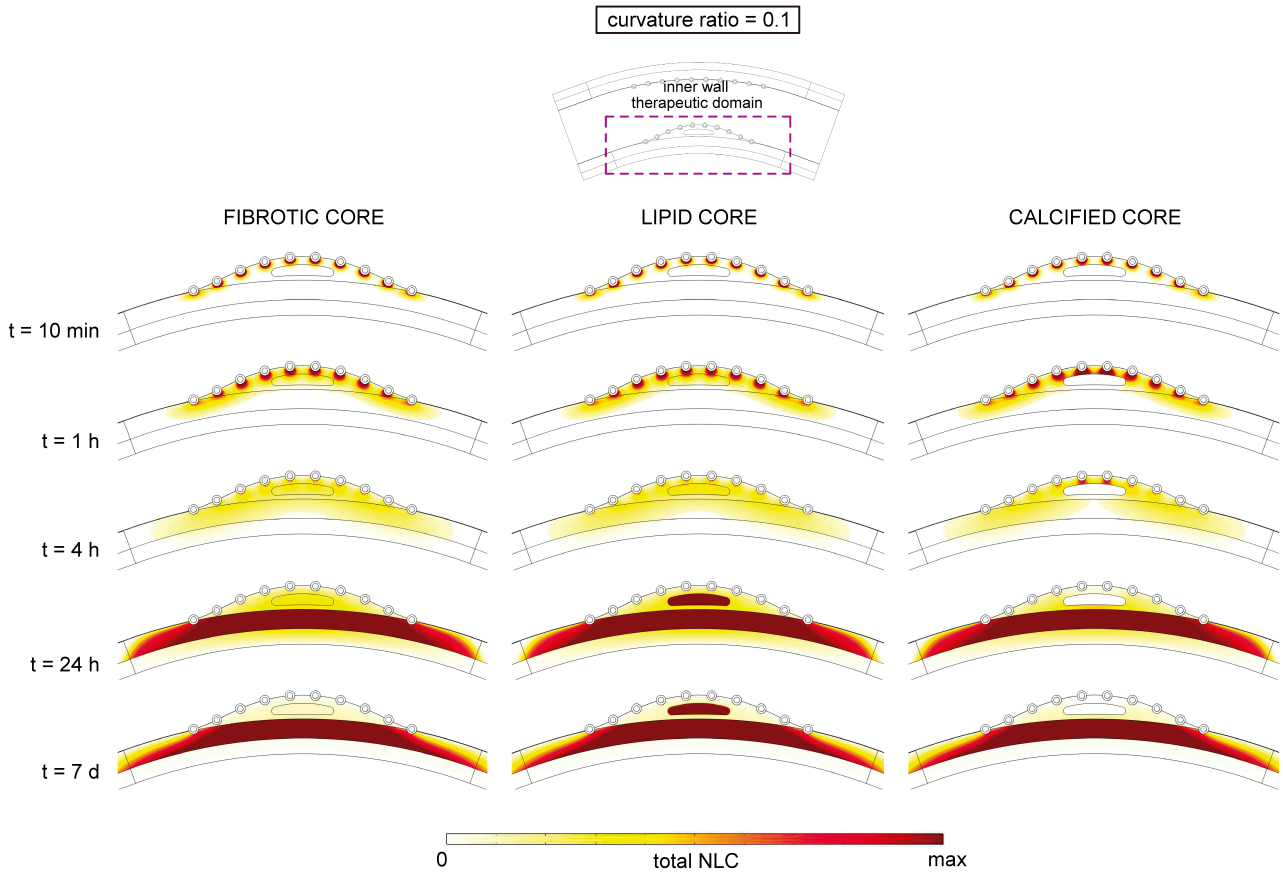

Fig. S22 Spatial variation of total NLC of sirolimus, calculated as $(c_i + b_i^s + b_i^{ns})/C_0$, in the inner wall of a curved artery ($\kappa = 0.1$) under unhealthy conditions (in presence of plaque) at five different time points (t = 10 min, t = 1 hour, t = 4 hours, t = 24 hours and t = 7 days). For each time point the same colour scale is used for both cases. The maximum values of total NLC of sirolimus for each time point are the following: max = $9.17 \cdot 10^{-2}$ at t = 10 min; max = $8.44 \cdot 10^{-2}$ at t = 1 h; max = $3.55 \cdot 10^{-2}$ at t = 4 h; max = $5.03 \cdot 10^{-3}$ at t = 24 h and; max = $2.53 \cdot 10^{-3}$ at t = 7 d. Tables with the maximum values at each time point for all cases considered may be found in Section S3 (Table S2) of this Supplementary Material.

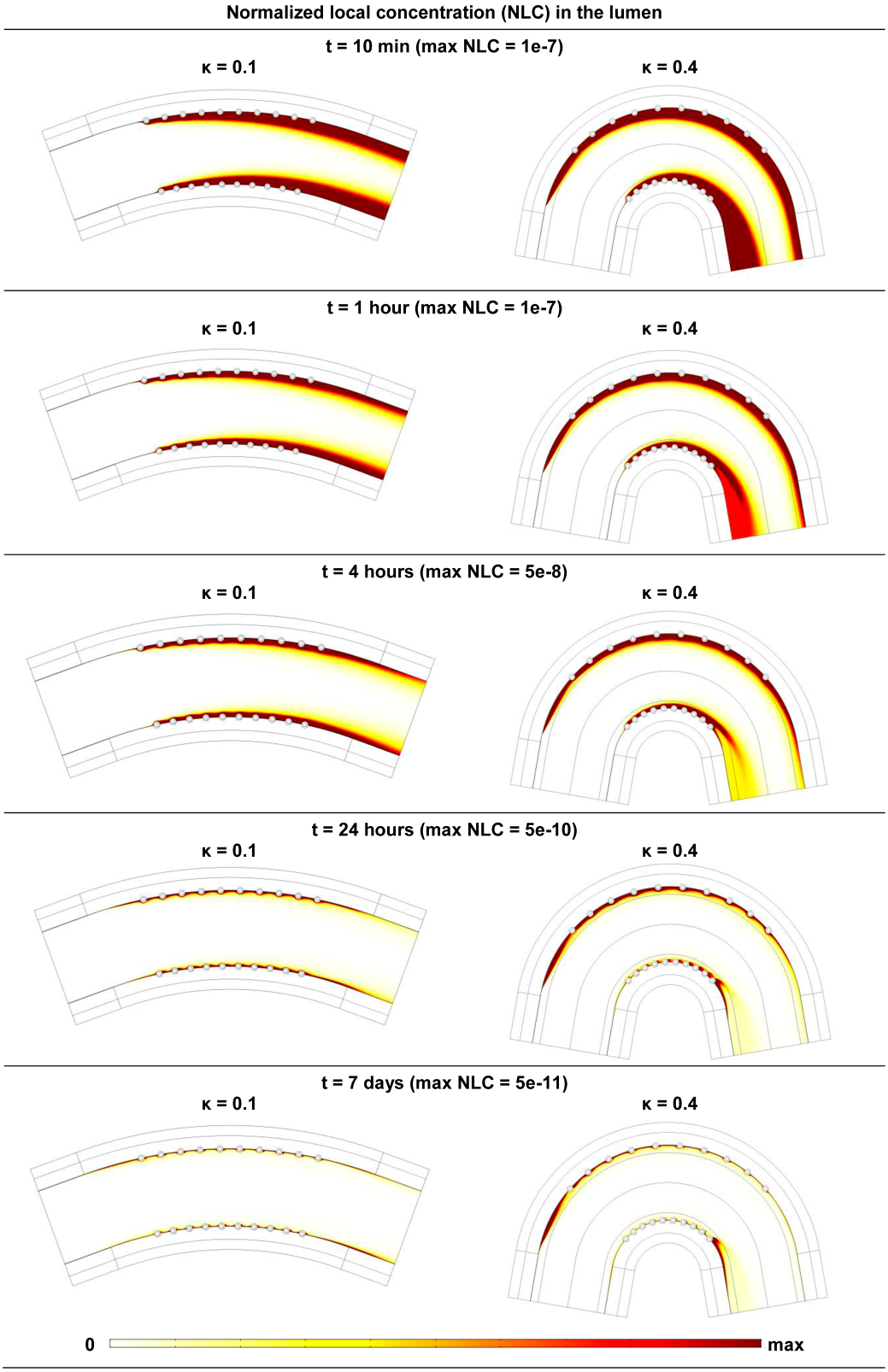

Fig. S23 Spatial variation of total (free) NLC of sirolimus, calculated as c_l/C_0, in the lumen for two different curvature ratios ($\kappa = 0.1$, corresponding to an average curvature and $\kappa = 0.4$, corresponding to a maximum curvature) under healthy conditions at five different time points (t = 10 min, t = 1 hour, t = 4 hours, t = 24 hours and t = 7 days). For each time point the same colour scale is used for both cases. The maximum values of total NLC of sirolimus for each time point are the following: max = $1 \cdot 10^{-7}$ at t = 10 min; max = $1 \cdot 10^{-7}$ at t = 1 h; max = $5 \cdot 10^{-8}$ at t = 4 h; max = $5 \cdot 10^{-10}$ at t = 24 h and; max = $5 \cdot 10^{-11}$ at t = 7 d.

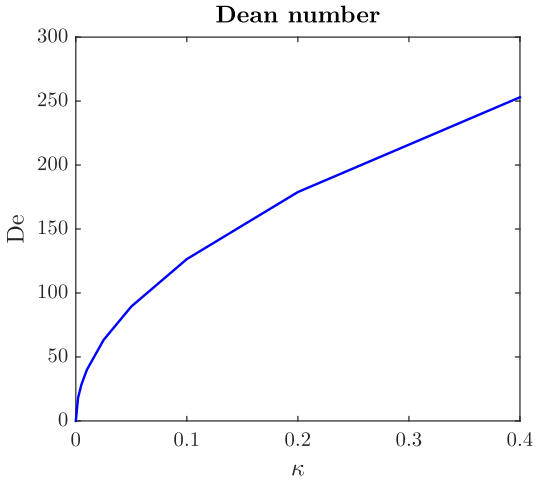

Fig. S24 Variation of the Dean number (De) for the flow in the straight artery ($\kappa = 0$) and in the curved vessel ($\kappa = 0.025 - 0.4$).

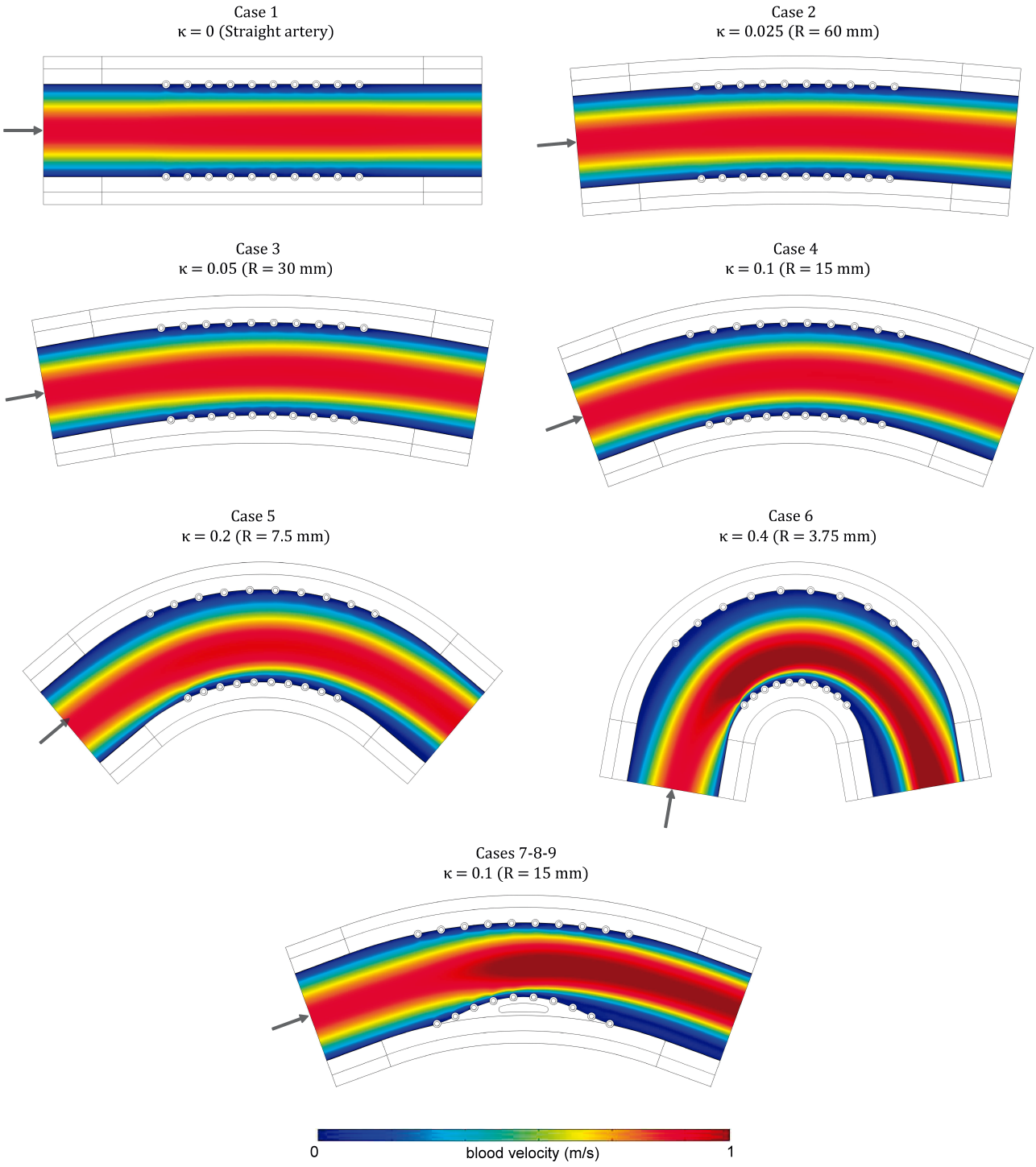

Fig. S25 Fuid flow pattern in the lumen for the straight artery ($\kappa = 0$) and for five different degrees of arterial curvature ($\kappa = 0.025 - 0.4$). The arrow indicates the inlet.

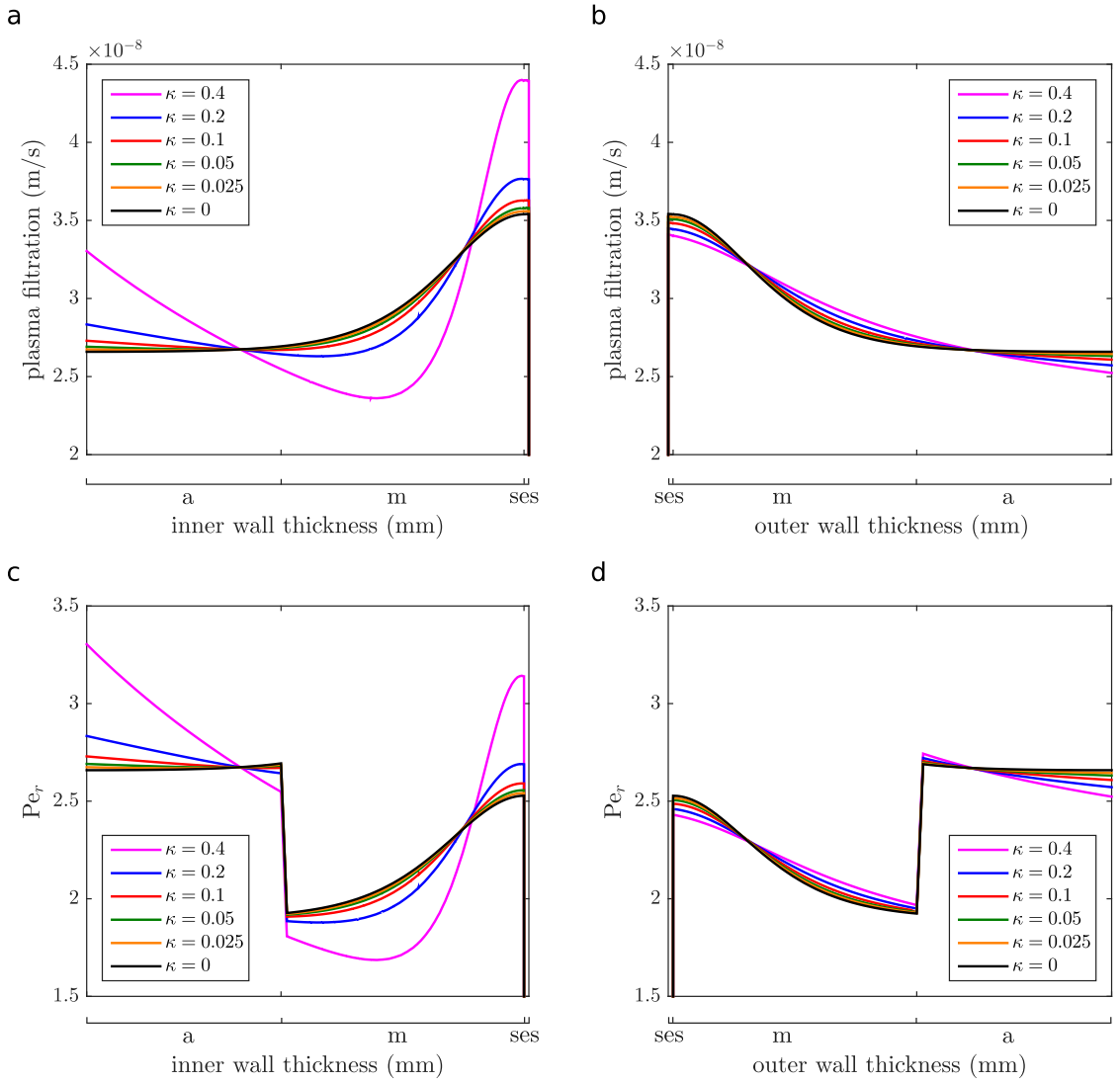

Fig. S26 Magnitude of the radial component of the plasma filtration (a, b) and radial Peclet number variation (c, d) in the inner and the outer wall of the artery. The results are shown for the healthy straight model ($\kappa = 0$) and for five different degrees of arterial curvature ($\kappa = 0.025 - 0.4$) in a radial section between the middle stent struts.

Table S1 Maximum normalised local concentrations (NLC) of sirolimus in each layer of the arterial wall for the straight segment ($\kappa = 0$) and for five different cases of arterial curvature ($\kappa = 0.025 - 0.4$) under healthy conditions (without plaque), at six different time points after stent implantation. Bold values in this table for a given time indicate the absolute maximum NLC of sirolimus in every case at the same time. They correspond to the 'max' values which appear in the legend in Figs. S8 - S13 which can be found in this supplementary material.

CASE 1. Healthy arterial wall. Straight segment ($\kappa = 0$)

max. value at	t = 10 min	t = 1 h	t = 4 h	t = 24 h	t = 7 d	t = 30 d
Total NLC in the SES (c_{ses})	$7.00{\cdot}10^{-3}$	$2.64{\cdot}10^{-3}$	$6.84{\cdot}10^{-4}$	$9.63{\cdot}10^{-7}$	$4.75{\cdot}10^{-8}$	$2.33{\cdot}10^{-9}$
Free NLC in the media (c_m)	$4.89{\cdot}10^{-2}$	$2.48{\cdot}10^{-2}$	$1.84{\cdot}10^{-2}$	$2.24{\cdot}10^{-4}$	$1.65{\cdot}10^{-5}$	$7.00{\cdot}10^{-7}$
S Bound NLC in the media (b_m^s)	$3.30{\cdot}10^{-5}$	$3.30{\cdot}10^{-5}$	$3.30{\cdot}10^{-5}$	$3.30{\cdot}10^{-5}$	$3.30{\cdot}10^{-5}$	$3.29{\cdot}10^{-5}$
NS Bound NLC in the media (b_m^{ns})	$3.63{\cdot}10^{-3}$	$3.63{\cdot}10^{-3}$	$3.62{\cdot}10^{-3}$	$3.25{\cdot}10^{-3}$	$1.41{\cdot}10^{-3}$	$9.51{\cdot}10^{-5}$
Total NLC in the media ($c_m + b_m^s + b_m^{ns}$)	$5.26{\cdot}10^{-2}$	$2.84{\cdot}10^{-2}$	$2.20{\cdot}10^{-2}$	$3.51{\cdot}10^{-3}$	$1.46{\cdot}10^{-3}$	$1.28{\cdot}10^{-4}$
Total NLC in the adventitia (c_a)	$4.04{\cdot}10^{-21}$	$1.11{\cdot}10^{-2}$	$1.88{\cdot}10^{-2}$	$2.24{\cdot}10^{-4}$	$1.64{\cdot}10^{-5}$	$6.95{\cdot}10^{-7}$

CASE 2. Healthy arterial wall. Curved segment ($\kappa = 0.025$)

max. value at	t = 10 min	t = 1 h	t = 4 h	t = 24 h	t = 7 d	t = 30 d
Total NLC in the SES (c_{ses})	$7.09{\cdot}10^{-3}$	$2.67{\cdot}10^{-3}$	$6.90{\cdot}10^{-4}$	$9.82{\cdot}10^{-7}$	$4.87{\cdot}10^{-8}$	$2.42{\cdot}10^{-9}$
Free NLC in the media (c_m)	$4.89{\cdot}10^{-2}$	$2.51{\cdot}10^{-2}$	$1.90{\cdot}10^{-2}$	$2.26{\cdot}10^{-4}$	$1.67{\cdot}10^{-5}$	$7.18{\cdot}10^{-7}$
S Bound NLC in the media (b_m^s)	$3.30{\cdot}10^{-5}$	$3.30{\cdot}10^{-5}$	$3.30{\cdot}10^{-5}$	$3.30{\cdot}10^{-5}$	$3.30{\cdot}10^{-5}$	$3.29{\cdot}10^{-5}$
NS Bound NLC in the media (b_m^{ns})	$3.63{\cdot}10^{-3}$	$3.63{\cdot}10^{-3}$	$3.63{\cdot}10^{-3}$	$3.26{\cdot}10^{-3}$	$1.42{\cdot}10^{-3}$	$9.76{\cdot}10^{-5}$
Total NLC in the media ($c_m + b_m^s + b_m^{ns}$)	$5.26{\cdot}10^{-2}$	$2.87{\cdot}10^{-2}$	$2.27{\cdot}10^{-2}$	$3.52{\cdot}10^{-3}$	$1.47{\cdot}10^{-3}$	$1.31{\cdot}10^{-4}$
Total NLC in the adventitia (c_a)	$4.39{\cdot}10^{-21}$	$1.15{\cdot}10^{-2}$	$1.95{\cdot}10^{-2}$	$2.27{\cdot}10^{-4}$	$1.66{\cdot}10^{-5}$	$7.14{\cdot}10^{-7}$

CASE 3. Healthy arterial wall. Curved segment ($\kappa = 0.05$)

max. value at	t = 10 min	t = 1 h	t = 4 h	t = 24 h	t = 7 d	t = 30 d
Total NLC in the SES (c_{ses})	$7.07{\cdot}10^{-3}$	$2.66{\cdot}10^{-3}$	$6.86{\cdot}10^{-4}$	$9.76{\cdot}10^{-7}$	$5.01{\cdot}10^{-8}$	$2.52{\cdot}10^{-9}$
Free NLC in the media (c_m)	$4.90{\cdot}10^{-2}$	$2.54{\cdot}10^{-2}$	$1.98{\cdot}10^{-2}$	$2.28{\cdot}10^{-4}$	$1.68{\cdot}10^{-5}$	$7.39{\cdot}10^{-7}$
S Bound NLC in the media (b_m^s)	$3.30{\cdot}10^{-5}$	$3.30{\cdot}10^{-5}$	$3.30{\cdot}10^{-5}$	$3.30{\cdot}10^{-5}$	$3.30{\cdot}10^{-5}$	$3.29{\cdot}10^{-5}$
NS Bound NLC in the media (b_m^{ns})	$3.63{\cdot}10^{-3}$	$3.63{\cdot}10^{-3}$	$3.63{\cdot}10^{-3}$	$3.26{\cdot}10^{-3}$	$1.43{\cdot}10^{-3}$	$1.00{\cdot}10^{-4}$
Total NLC in the media ($c_m + b_m^s + b_m^{ns}$)	$5.27{\cdot}10^{-2}$	$2.90{\cdot}10^{-2}$	$2.34{\cdot}10^{-2}$	$3.52{\cdot}10^{-3}$	$1.48{\cdot}10^{-3}$	$1.34{\cdot}10^{-4}$
Total NLC in the adventitia (c_a)	$4.12{\cdot}10^{-21}$	$1.21{\cdot}10^{-2}$	$2.02{\cdot}10^{-2}$	$2.29{\cdot}10^{-4}$	$1.67{\cdot}10^{-5}$	$7.35{\cdot}10^{-7}$

CASE 4. Healthy arterial wall. Curved segment ($\kappa = 0.1$)

max. value at	t = 10 min	t = 1 h	t = 4 h	t = 24 h	t = 7 d	t = 30 d
Total NLC in the SES (c_{ses})	$7.20{\cdot}10^{-3}$	$2.70{\cdot}10^{-3}$	$6.99{\cdot}10^{-4}$	$9.93{\cdot}10^{-7}$	$5.32{\cdot}10^{-8}$	$2.77{\cdot}10^{-9}$
Free NLC in the media (c_m)	$4.93{\cdot}10^{-2}$	$2.62{\cdot}10^{-2}$	$2.14{\cdot}10^{-2}$	$2.33{\cdot}10^{-4}$	$1.71{\cdot}10^{-5}$	$7.92{\cdot}10^{-7}$
S Bound NLC in the media (b_m^s)	$3.30{\cdot}10^{-5}$	$3.30{\cdot}10^{-5}$	$3.30{\cdot}10^{-5}$	$3.30{\cdot}10^{-5}$	$3.30{\cdot}10^{-5}$	$3.29{\cdot}10^{-5}$
NS Bound NLC in the media (b_m^{ns})	$3.63{\cdot}10^{-3}$	$3.63{\cdot}10^{-3}$	$3.63{\cdot}10^{-3}$	$3.27{\cdot}10^{-3}$	$1.44{\cdot}10^{-3}$	$1.07{\cdot}10^{-4}$
Total NLC in the media ($c_m + b_m^s + b_m^{ns}$)	$5.29{\cdot}10^{-2}$	$2.98{\cdot}10^{-2}$	$2.51{\cdot}10^{-2}$	$3.53{\cdot}10^{-3}$	$1.49{\cdot}10^{-3}$	$1.41{\cdot}10^{-4}$
Total NLC in the adventitia (c_a)	$4.09{\cdot}10^{-21}$	$1.32{\cdot}10^{-2}$	$2.19{\cdot}10^{-2}$	$2.34{\cdot}10^{-4}$	$1.70{\cdot}10^{-5}$	$7.87{\cdot}10^{-7}$

CASE 5. Healthy arterial wall. Curved segment ($\kappa = 0.2$)

max. value at	t = 10 min	t = 1 h	t = 4 h	t = 24 h	t = 7 d	t = 30 d
Total NLC in the SES (c_{ses})	$7.81{\cdot}10^{-3}$	$2.92{\cdot}10^{-3}$	$7.53{\cdot}10^{-4}$	$1.22{\cdot}10^{-6}$	$9.80{\cdot}10^{-8}$	$3.93{\cdot}10^{-9}$
Free NLC in the media (c_m)	$5.04{\cdot}10^{-2}$	$2.83{\cdot}10^{-2}$	$2.57{\cdot}10^{-2}$	$2.45{\cdot}10^{-4}$	$1.79{\cdot}10^{-5}$	$9.48{\cdot}10^{-7}$
S Bound NLC in the media (b_m^s)	$3.63{\cdot}10^{-3}$	$3.63{\cdot}10^{-3}$	$3.63{\cdot}10^{-3}$	$3.28{\cdot}10^{-3}$	$1.48{\cdot}10^{-3}$	$1.27{\cdot}10^{-4}$
NS Bound NLC in the media (b_m^{ns})	$3.30{\cdot}10^{-5}$	$3.30{\cdot}10^{-5}$	$3.30{\cdot}10^{-5}$	$3.30{\cdot}10^{-5}$	$3.30{\cdot}10^{-5}$	$3.29{\cdot}10^{-5}$
Total NLC in the media ($c_m + b_m^s + b_m^{ns}$)	$5.41{\cdot}10^{-2}$	$3.19{\cdot}10^{-2}$	$2.93{\cdot}10^{-2}$	$3.56{\cdot}10^{-3}$	$1.53{\cdot}10^{-3}$	$1.61{\cdot}10^{-4}$
Total NLC in the adventitia (c_a)	$4.29{\cdot}10^{-21}$	$1.58{\cdot}10^{-2}$	$2.63{\cdot}10^{-2}$	$2.47{\cdot}10^{-4}$	$1.78{\cdot}10^{-5}$	$9.42{\cdot}10^{-7}$

CASE 6. Healthy arterial wall. Curved segment ($\kappa = 0.4$)

max. value at	t = 10 min	t = 1 h	t = 4 h	t = 24 h	t = 7 d	t = 30 d
Total NLC in the SES (c_{ses})	$1.02{\cdot}10^{-2}$	$3.77{\cdot}10^{-3}$	$9.73{\cdot}10^{-4}$	$1.37{\cdot}10^{-6}$	$1.06{\cdot}10^{-7}$	$5.92{\cdot}10^{-9}$
Free NLC in the media (c_m)	$5.86{\cdot}10^{-2}$	$3.79{\cdot}10^{-2}$	$4.19{\cdot}10^{-2}$	$2.88{\cdot}10^{-4}$	$2.24{\cdot}10^{-5}$	$1.29{\cdot}10^{-6}$
S Bound NLC in the media (b_m^s)	$3.30{\cdot}10^{-5}$	$3.30{\cdot}10^{-5}$	$3.30{\cdot}10^{-5}$	$3.30{\cdot}10^{-5}$	$3.30{\cdot}10^{-5}$	$3.30{\cdot}10^{-5}$
NS Bound NLC in the media (b_m^{ns})	$3.63{\cdot}10^{-3}$	$3.63{\cdot}10^{-3}$	$3.63{\cdot}10^{-3}$	$3.33{\cdot}10^{-3}$	$1.68{\cdot}10^{-3}$	$1.71{\cdot}10^{-4}$
Total NLC in the media ($c_m + b_m^s + b_m^{ns}$)	$\mathbf{6.23 \cdot 10^{-2}}$	$\mathbf{4.16 \cdot 10^{-2}}$	$\mathbf{4.56 \cdot 10^{-2}}$	$\mathbf{3.65 \cdot 10^{-3}}$	$\mathbf{1.74 \cdot 10^{-3}}$	$\mathbf{2.05 \cdot 10^{-4}}$
Total NLC in the adventitia (c_a)	$2.67{\cdot}10^{-23}$	$2.41{\cdot}10^{-2}$	$4.28{\cdot}10^{-2}$	$2.94{\cdot}10^{-4}$	$2.22{\cdot}10^{-5}$	$1.28{\cdot}10^{-6}$

Table S2 Maximum normalised local concentrations (NLC) of sirolimus in each region of the diseased arterial wall (with plaque) in a curved segment ($\kappa = 0.1$), at six different time points after stent implantation. Bold values in this table for a given time indicate the absolute maximum NLC of sirolimus in every case at the same time. They correspond to the 'max' values which appear in the legend in Fig. S22 which can be found in this supplementary material.

CASE 7. Diseased arterial wall (Fibrotic core). Curved segment ($\kappa = 0.1$)

max. value at	t = 10 min	t = 1 h	t = 4 h	t = 24 h	t = 7 d	t = 30 d
Total NLC in the SES (c_{ses})	$6.64{\cdot}10^{-3}$	$2.49{\cdot}10^{-3}$	$6.44{\cdot}10^{-4}$	$5.61{\cdot}10^{-6}$	$3.39{\cdot}10^{-7}$	$4.30{\cdot}10^{-8}$
Free NLC in the plaque (c_{i2})	$8.75{\cdot}10^{-2}$	$5.76{\cdot}10^{-2}$	$2.37{\cdot}10^{-2}$	$1.34{\cdot}10^{-3}$	$3.61{\cdot}10^{-5}$	$7.52{\cdot}10^{-6}$
Bound NLC in the plaque (b_{i2})	$3.00{\cdot}10^{-4}$	$3.00{\cdot}10^{-4}$	$3.00{\cdot}10^{-4}$	$2.94{\cdot}10^{-4}$	$1.74{\cdot}10^{-4}$	$6.73{\cdot}10^{-5}$
Total NLC in the plaque ($c_{i2} + b_{i2}$)	$8.78{\cdot}10^{-2}$	$5.79{\cdot}10^{-2}$	$2.40{\cdot}10^{-2}$	$1.63{\cdot}10^{-3}$	$2.10{\cdot}10^{-4}$	$7.48{\cdot}10^{-5}$
Free NLC in the media (c_m)	$4.89{\cdot}10^{-2}$	$3.17{\cdot}10^{-2}$	$1.60{\cdot}10^{-2}$	$1.43{\cdot}10^{-3}$	$4.29{\cdot}10^{-5}$	$9.09{\cdot}10^{-6}$
S Bound NLC in the media (b_m^s)	$3.30{\cdot}10^{-5}$	$3.30{\cdot}10^{-5}$	$3.30{\cdot}10^{-5}$	$3.30{\cdot}10^{-5}$	$3.30{\cdot}10^{-5}$	$3.30{\cdot}10^{-5}$
NS Bound NLC in the media (b_m^{ns})	$3.63{\cdot}10^{-3}$	$3.63{\cdot}10^{-3}$	$3.62{\cdot}10^{-3}$	$3.57{\cdot}10^{-3}$	$2.26{\cdot}10^{-3}$	$9.40{\cdot}10^{-4}$
Total NLC in the media ($c_m + b_m^s + b_m^{ns}$)	$5.26{\cdot}10^{-2}$	$3.54{\cdot}10^{-2}$	$1.96{\cdot}10^{-2}$	$\mathbf{5.03 \cdot 10^{-3}}$	$2.34{\cdot}10^{-3}$	$9.82{\cdot}10^{-4}$
Total NLC in the adventitia (c_a)	$3.84{\cdot}10^{-21}$	$9.34{\cdot}10^{-3}$	$1.63{\cdot}10^{-2}$	$1.32{\cdot}10^{-3}$	$3.78{\cdot}10^{-5}$	$8.00{\cdot}10^{-6}$

CASE 8. Diseased arterial wall (Lipid core). Curved segment ($\kappa = 0.1$)

max. value at	t = 10 min	t = 1 h	t = 4 h	t = 24 h	t = 7 d	t = 30 d
Total NLC in the SES (c_{ses})	$6.64{\cdot}10^{-3}$	$2.49{\cdot}10^{-3}$	$6.44{\cdot}10^{-4}$	$5.56{\cdot}10^{-6}$	$3.40{\cdot}10^{-7}$	$4.41{\cdot}10^{-8}$
Free NLC in the plaque (c_{i2})	$8.75{\cdot}10^{-2}$	$5.75{\cdot}10^{-2}$	$2.35{\cdot}10^{-2}$	$1.31{\cdot}10^{-3}$	$4.36{\cdot}10^{-5}$	$9.49{\cdot}10^{-6}$
Bound NLC in the plaque (b_{i2})	$3.65{\cdot}10^{-3}$	$3.66{\cdot}10^{-3}$	$3.65{\cdot}10^{-3}$	$3.58{\cdot}10^{-3}$	$2.22{\cdot}10^{-3}$	$9.09{\cdot}10^{-4}$
Total NLC in the plaque ($c_{i2} + b_{i2}$)	$8.78{\cdot}10^{-2}$	$5.78{\cdot}10^{-2}$	$2.38{\cdot}10^{-2}$	$4.77{\cdot}10^{-3}$	$2.26{\cdot}10^{-3}$	$9.17{\cdot}10^{-4}$
Free NLC in the media (c_m)	$4.89{\cdot}10^{-2}$	$3.17{\cdot}10^{-2}$	$1.60{\cdot}10^{-2}$	$1.40{\cdot}10^{-3}$	$4.69{\cdot}10^{-5}$	$1.03{\cdot}10^{-5}$
S Bound NLC in the media (b_m^s)	$3.66{\cdot}10^{-3}$	$3.66{\cdot}10^{-3}$	$3.65{\cdot}10^{-3}$	$3.59{\cdot}10^{-3}$	$2.36{\cdot}10^{-3}$	$3.43{\cdot}10^{-7}$
NS Bound NLC in the media (b_m^{ns})	$3.30{\cdot}10^{-5}$	$3.30{\cdot}10^{-5}$	$3.30{\cdot}10^{-5}$	$3.30{\cdot}10^{-5}$	$3.30{\cdot}10^{-5}$	$3.30{\cdot}10^{-5}$
Total NLC in the media ($c_m + b_m^s + b_m^{ns}$)	$5.26{\cdot}10^{-2}$	$3.54{\cdot}10^{-2}$	$1.96{\cdot}10^{-2}$	$5.00{\cdot}10^{-3}$	$2.42{\cdot}10^{-3}$	$1.08{\cdot}10^{-3}$
Total NLC in the adventitia (c_a)	$3.83{\cdot}10^{-21}$	$9.34{\cdot}10^{-3}$	$1.63{\cdot}10^{-2}$	$1.29{\cdot}10^{-3}$	$4.04{\cdot}10^{-5}$	$8.91{\cdot}10^{-6}$

CASE 9. Diseased arterial wall (Calcified core). Curved segment ($\kappa = 0.1$)

max. value at	t = 10 min	t = 1 h	t = 4 h	t = 24 h	t = 7 d	t = 30 d
Total NLC in the SES (c_{ses})	$6.64{\cdot}10^{-3}$	$2.49{\cdot}10^{-3}$	$6.44{\cdot}10^{-4}$	$5.13{\cdot}10^{-6}$	$3.40{\cdot}10^{-7}$	$4.49{\cdot}10^{-8}$
Free NLC in the plaque (c_{i2})	$9.14{\cdot}10^{-2}$	$8.41{\cdot}10^{-2}$	$3.52{\cdot}10^{-2}$	$1.42{\cdot}10^{-3}$	$5.34{\cdot}10^{-5}$	$1.22{\cdot}10^{-5}$
Bound NLC in the plaque (b_{i2})	$3.00{\cdot}10^{-4}$	$3.00{\cdot}10^{-4}$	$3.00{\cdot}10^{-4}$	$2.94{\cdot}10^{-4}$	$2.01{\cdot}10^{-4}$	$9.63{\cdot}10^{-5}$
Total NLC in the plaque ($c_{i2} + b_{i2}$)	$\mathbf{9.17 \cdot 10^{-2}}$	$\mathbf{8.44 \cdot 10^{-2}}$	$\mathbf{3.55 \cdot 10^{-2}}$	$1.71{\cdot}10^{-3}$	$2.55{\cdot}10^{-4}$	$1.08{\cdot}10^{-4}$
Free NLC in the media (c_m)	$4.89{\cdot}10^{-2}$	$3.17{\cdot}10^{-2}$	$1.60{\cdot}10^{-2}$	$1.39{\cdot}10^{-3}$	$5.34{\cdot}10^{-5}$	$1.23{\cdot}10^{-5}$
S Bound NLC in the media (b_m^s)	$3.30{\cdot}10^{-5}$	$3.30{\cdot}10^{-5}$	$3.30{\cdot}10^{-5}$	$3.30{\cdot}10^{-5}$	$3.30{\cdot}10^{-5}$	$3.30{\cdot}10^{-5}$
NS Bound NLC in the media (b_m^{ns})	$3.63{\cdot}10^{-3}$	$3.63{\cdot}10^{-3}$	$3.62{\cdot}10^{-3}$	$3.56{\cdot}10^{-3}$	$2.44{\cdot}10^{-3}$	$1.17{\cdot}10^{-3}$
Total NLC in the media ($c_m + b_m^s + b_m^{ns}$)	$5.26{\cdot}10^{-2}$	$3.54{\cdot}10^{-2}$	$1.96{\cdot}10^{-2}$	$4.99{\cdot}10^{-3}$	$\mathbf{2.53 \cdot 10^{-3}}$	$\mathbf{1.21 \cdot 10^{-3}}$
Total NLC in the adventitia (c_a)	$3.83{\cdot}10^{-21}$	$9.34{\cdot}10^{-3}$	$1.63{\cdot}10^{-2}$	$1.10{\cdot}10^{-3}$	$4.25{\cdot}10^{-5}$	$9.71{\cdot}10^{-6}$